Scholarship@Western

Digitized Theses   Digitized Special Collections

2011

VOLTAGE-SENSITIVE DYE IMAGING OF RAT PIRIFORM CORTEX BEFORE AND AFTER KINDLING

Zeinab Biriandian

Follow this and additional works at: https://ir.lib.uwo.ca/digitizedtheses

VOLTAGE-SENSITIVE DYE IMAGING OF RAT PIRIFORM CORTEX BEFORE
AND AFTER KINDLING

(Spine title: Voltage-Sensitive Dye Imaging of Piriform Cortex)

(Thesis format: Monograph)

by

Zeinab Birjandian

Graduate Program in Physiology

A thesis submitted in partial fulfillment
of the requirements for the degree of
Master of Science

The School of Graduate and Postdoctoral Studies
The University of Western Ontario
London, Ontario, Canada

CERTIFICATE OF EXAMINATION

Supervisor

_____

Dr. Michael O. Poulter

Supervisory Committee

_____

Dr. Richard S. McLachlan

_____

Dr. Michael Jackson

_____

Dr. Marco Prado

Examiners

_____

Dr. Stephen Sims

_____

Dr. John F. MacDonald

_____

Dr. Mandar S. Jog

The thesis by

Zeinab Birjandian

entitled:

VOLTAGE-SENSITIVE DYE IMAGING OF RAT PIRIFORM CORTEX BEFORE AND AFTER KINDLING

is accepted in partial fulfillment of the
requirements for the degree of
Master of Science

Date_____   _____
                                      Chair of the Thesis Examination Board

Abstract

To determine the role of inhibitory cells in the propagation of activity in the rat piriform cortex (PC) before and after kindling, we used voltage-sensitive dye imaging technique to follow the membrane potential changes in three layers of the PC after stimulating the lateral olfactory tract (LOT) with beta and gamma frequencies. Stimulation of LOT was followed by propagation of excitatory (in layer II) and inhibitory responses (in layer III) through the PC. Decreasing the inhibition by applying gabazine, a $GABA_A$- receptor antagonist, decreased the inhibitory responses and increased the excitatory responses in the control rats; however, it did not affect the excitatory and inhibitory responses in the kindled rats. Furthermore, cutting the slice below the layer II decreased the both responses. Thus, we concluded that disinhibition of layer III interneurons is necessary for principle cells firing and kindling can result in seizures by increasing disinhibition in layer III of PC.

Keywords: piriform cortex, interneuron, voltage-sensitive dye imaging, kindling, disinhibition, oscillation

Acknowledgments

This research project would not have been possible without the support of many people. I would like to express my gratitude to my supervisor, Prof. Dr. Michael O. Poulter who was abundantly helpful and offered invaluable assistance, support and guidance. Deepest gratitude are also due to the members of the advisory committee, Dr. Richard S. McLachlan, Dr. Brian Corneil, Dr. Marco Prado and Dr. Michael Jackson, without whose knowledge and assistance this study would not have been successful.

Special thanks also to all my friends, Cezar Gavrilovici, Arash Kia, Fiona Simpson, Chakravanthi Narla, Michele Everest and Deborah Anderson for their invaluable assistance during this project.

I would also like to express my heartfelt thanks to my beloved family and especially my husband, Omid Mola, for their love and encouragements. Without my husband's supports, I would not have finished this degree.

Table of Contents

List of Figures

List of Abbreviations

AD   after discharge
ADT   after discharge threshold
AMPA   α-amino-3-hydroxy-5-methyl-4-isoxazolepropionic acid
ANEPPS   aminonaphthethenyl pyridinium propylsulfonate
BLA   basolateral amygdala
CA1   cornus ammonis
CB   calbindin
CCD   charge coupled device
ChCs   chandelier cells
CMOS   complementary metal oxide semiconductor
CR   calretinin
DBCs   double bouquet cells
DG   deoxyglucose
EPSPs   excitatory postsynaptic potentials
$GABA_A$ gamma-amino butyric acid type A receptor
IN   interneuron
IPSPs   inhibitory postsynaptic potentials
LFPs   local field potentials
LOT   lateral olfactory tract
MEA   multielectrode array
nM   nano molar
NMDA   N-methyl-D-aspartate
OB   olfactory bulb
PV   paravalbumin
SPs   superficial pyramidal cells
TLE   temporal lobe epilepsy
TTX   tetrodotoxin

1. Introduction

One of the most remarkable aspects of the human body is the human brain, which is an assembly of billions of neurons that are interconnected in a highly complex yet organized manner. For the brain to function properly this neural network must connect in a manner that supports the generation of brain rhythms that are associated with various behaviours (for example memory formation and sleep). Each part of the brain can be conceptualized as a group of computers that process information like a distributed network (as opposed to parallel processing) that interpret the differing stimuli the brain receives from the environment. Importantly the eventual behavioural output relies on the precise correlation and synchrony between all these distributed structures. In particular, many studies have shown that cognitive abilities in human beings such as working memory or conscious processing of stimuli need very high integration of these distributed neuronal activities (Singer, 1999;Schnitzler & Gross, 2005;Varela et al., 2001).

Neurons are the functional units of central nervous system. In the mammalian cerebral cortex there are two major classes of neurons known as spiny neurons and aspiny non-pyramidal neurons. Spiny neurons are further divided into pyramidal cells and spiny non-pyramidal cells. Pyramidal cells are the most abundant cell types in all parts of cerebral cortex and form asymmetric excitatory synapses on other neurons (Colonnier & O'Kusky, 1981). Pyramidal cells possess typical characteristics that differentiate them from other cortical neurons, these include: ovoid or pyramidal shape soma, apical dendrite arises from the upper pole and directs radially toward the pia mater and the axons that come from the base of the cell or from the origin of a basal dendrite. Axons

1

give off many collaterals throughout the cortex. All dendritic surfaces are covered with spines except the proximal part arising from the somata (Feldman, 1984). Interneurons, which consist of spiny and aspiny non-pyramidal cells are the main inhibitory cell type in the cerebral cortex. Different morphological types of interneurons can be found depending on the species and cortical area they are located (Lund, 1984;Fairen et al., 1984). Interneurons have been classified into distinct groups based on different characteristics such as morphological, functional, physiological and molecular features (Bayraktar et al., 2000;Porter et al., 1998;Rozov et al., 2001). Neocortical interneurons are divided into many groups according to their dendritic and axonal arborizations. Basket cells are large multipolar cells and their axons form a basket–like appearance around the somata of target cells. Basket cells target somata and proximal dendrites of pyramidal cells as well as other interneurons. They are mostly positive for two kinds of calcium binding proteins, calbindin and parvalbumin. Chandelier cells (ChCs) are another group of interneurons. Terminal axons of chandelier cells form short vertical row of boutons resembling candlesticks (Szentagothai & Arbib, 1974;Ascoli et al., 2008). ChCs are fast spiking neurons that never target interneurons. Because of their inhibitory synapses on axon initial segment of pyramidal cells, ChCs are considered the most powerful inhibitory neurons (Jones, 1975;Del Rio & DeFelipe, 1994;Del Rio & DeFelipe, 1994;Del Rio & DeFelipe, 1997;Gabbott & Bacon, 1996). This is important because axon initial segment has a high-density of voltage-gated sodium channels that lowers the threshold for action potential initiation. Thus, axon initial segment is thought to be the most strategic region to generate the action potential (Catterall, 1981;Wollner & Catterall, 1986). Martinotti cells (MCs) represent a group of interneurons with ovoid or

spindle somata and laterally extended dendrites. This extensive horizontal structure makes it possible for MCs to inhibit distal dendritic tufts of pyramidal neurons (Ramón y Cajal, 1911;Gabbott & Bacon, 1996). Most MC cells show a low threshold regular spiking pattern (Kawaguchi & Kubota, 1993). MCs are mostly connected with gap junctions and less frequently chemical synapses (Hestrin & Galarreta, 2005). The next group of interneurons is double-bouquet cells (DBCs), which show a bi-tufted dendritic shape and vertically descending axons. They mostly innervate dendrites with interlayer connections in neocortex. DBCs are functionally non-fast-spiking neurons (Kawaguchi & Kondo, 2002). Bipolar cells are another group of cells mostly found in layers II-VI. Their axons cross all layers and innervate mostly pyramidal cells (Markram et al., 2004). Bitufted cells also have the same distribution as bipolar cells with more extended axons, targeting other dendrites (Markram et al., 2004). Neurogliaform cells, which were first described by Ramon y Cajal (1911), are small cells with round somata (Kawaguchi & Kubota, 1997). The specific characteristic of neurogliaform cells is the formation of electrical synapses with each other as well as other types of interneurons, such as bipolar cells and ChCs. (Simon et al., 2005)

A complex network of axosomatic, axodendritic and axoaxonic synapses connect the excitatory and inhibitory cells and also the cells in each group. Immmunohistochemical studies indicate that GABAergic terminals form the majority of synapses on pyramidal cell somata (Ribak, 1978;Hendry et al., 1983). These inhibitory synapses located on the soma are optimal to inhibit the inputs arriving from all the cell dendrites (Jack, 1975). In addition the major synapses on axon initial segment of pyramidal cells are chandelier cells, which are known to be GABAergic (Freund et al.,

3

1983;Somogyi et al., 1985;DeFelipe et al., 1985). Interneurons are connected to other interneurons via both GABAergic synapses and gap junctions (Galarreta & Hestrin, 1999;Tamas et al., 2000). Interneurons also receive excitatory synapses from pyramidal cells via their high affinity sites for glutamate and kainate (Dingledine et al., 1999a). Pyramidal cells are interconnected by asymmetric excitatory synapses on dendritic shafts and spines of other principal cells (White & Hersch, 1981;White & Hersch, 1982;Porter & White, 1986).

Synaptic transmission through neurotransmitters is fundamental for information processing in the brain's complex networks. Neurotransmitters, either excitatory or inhibitory, are necessary for the synchronized activity of many excitable neurons in the central nervous system. Immunocytochemical studies have found several neurotransmitters in the cerebral cortex such as noradrenaline, gammma-amino butyric acid (GABA), glutamate, dopamine and neuropeptides (somatostatin, neuropeptide Y, vasoactive intestinal peptide, etc) (Jones, 1986;Benson et al., 1991). Moreover, L-glutamate and L-aspartate are the main excitatory amino acids commonly found in axon terminals of pyramidal cells and gamma-amino butyric acid (GABA) is the most abundant inhibitory neurotransmitter produced in interneurons (Emson & Lindvall, 1979;Conti et al., 1988). GABA containing cells form exclusively symmetric type synapses whereas glutamate containing terminals form asymmetric synapses (Ribak, 1978;Freund et al., 1983;Hendry et al., 1983;DeFelipe et al., 1985;Somogyi & Soltesz, 1986;Verney et al., 1990;Beaulieu & Somogyi, 1991;Ascoli et al., 2008;DeFelipe & Jones, 1992;Conti et al., 1989;Dori et al., 1989).

1.1 Pathophysiology of seizure disorders

Any perturbation in the level of neural excitability or synchrony can contribute to dysfunctional network activity, which is an underlying cause of many CNS disorders such as seizure (Cossart et al., 2001a;Cossart et al., 2005;Kamphuis et al., 1994). Traditionally, a seizure is defined as "a transient occurrence of pathophysiological behaviour that is due to abnormal and/or excessive synchronous neuronal activity in the brain" (Fisher et al., 2005). Seizures are typically divided into two main different types called partial and general. In partial or focal seizures the seizure activity usually starts from a local region of a cerebral hemisphere that subsequently may spread to other parts of the brain. It has been shown that some parts of the brain are more vulnerable than others to initiate the hyper synchrony. These include limbic structures in the mesial temporal lobe, especially the hippocampus, parahippocampal regions, subiculum, etorhinal cortex, and amygdala. Partial seizures are further sub classified into three groups, i.e. simple partial seizures, complex partial seizures, and partial seizures secondarily generalizing to clonic and/or tonic seizures. In generalized seizures, however, there is no evidence of focal onset, but essentially spreads over all or large parts of both cerebral hemispheres from onset. Based on epidemiological data, 40-50% of all epileptic patients suffer from the complex partial seizures with or without secondary generalization. The majority (70-85%) of complex partial seizures originate in the temporal lobes, particularly in hippocampus and amygdala, and termed as temporal lobe epilepsy (TLE) (Loscher & Schmidt, 1994;Engel & Pedley, 2008). Although epilepsies are diverse groups of disorders, all having common characteristics of hyperexcitability and synchrony, these classifications can often be overlapping.

The etiology of epilepsy includes the wide range of heterogeneous factors that can contribute to abrupt bursts of synchronous activity. These vary from structural damage (encephalitis, tumours and craniocerebral trauma) to abnormal metabolic states such as fever or sleep deprivation and genetic predispositions (Engel & Pedley, 2008). Despite intensive research in the epilepsy field, there are still many unanswered questions about fundamental mechanism of epilepsy. Experimentally, seizures can be produced by either reducing inhibitory activity or increasing excitatory activity of the brain networks. Thus, epilepsy has been conceptualized as being the result of an imbalance between synchronized inhibitory and excitatory neuronal fire (Cossart et al., 2001b;Cossart et al., 2005;Dinocourt et al., 2003;Fritschy et al., 1999;Gavrilovici et al., 2006;Kamphuis et al., 1994;Sloviter, 1987). This idea has resulted in development of new drugs targeting the inhibitory activity such as vigabatrin, which blocks GABA metabolism; thus raising its level in brain and theoretically counterbalances excess excitatory drive. However, the clinical results of these drugs have not often had the predicted clinical efficacy. Therefore, the idea of an imbalance of inhibition versus excitation may be overly simplistic.

1.2 Animal Models of Epilepsy

In order to study the underlying mechanisms of epilepsy scientists have employed animal models that attempt to mimic epilepsy (to varying degrees of success). There are basically three differing kinds of models. Those that use drugs to cause seizures, those where the genetic phenotype has been altered either by inbreeding or gene transfer and those that employ electrical stimulation (kindling) (Coulter et al., 2002).

1.2.1 Chemical Models

In these models, status epilepticus is induced in the subject animals by injecting chemical convulsants such as pilocarpine (cholinergic receptor agonist) and kainic acid (kainite receptor agonist). Animals then appear overtly normal for a period of time varying between 2 weeks and several months. At the end of this time, the animals begin to exhibit frequent spontaneous secondarily generalized seizures, which usually persist for the remainder of the life of the animal (Ben-Ari et al., 1979;Turski et al., 1983). Different pathological findings have been reported in these animal models. Hippocampal sclerosis and axonal sprouting are the main pathological features in chemical models. Hippocampal pathology in the chemical animal models is similar to the damage seen in patients with temporal lobe epilepsy (Ben-Ari, 1985;Cavalheiro et al., 1991;Sloviter, 1987;Turski et al., 1989). There are other convulsive chemicals that are less popular. These include: bicuculline a potent $GABA_A$-receptor inhibitor, cobalt-homocystein and flurothyl (bis-2, 2,2-triflurothyl ether) a convulsive gas (Meldrum & Horton, 1978;Walton & Treiman, 1988;Nevander et al., 1985).

1.2.2 Genetic Models

Two strains of fast-kindled and slow-kindled rats were developed by selective breeding of different strains based on their rates of amygdala kindling. Fast rats can achieve the last stage of kindling (stage5) with daily amygdala kindling in a week, whereas the slow rats reach the stage5 after 3 weeks of daily stimulation (Racine R. et al., 1999;Poulter et al., 1999). Another animal model of epilepsy are genetically epilepsy-

prone rats, which are susceptible to acoustically evoked convulsions (Faingold et al., 1991;Jobe et al., 1973). This strain exhibits convulsions when exposed to sound stimulus. Subcortical region disorders are responsible for seizure susceptibility in these animals (Chocholova, 1962). Mutant rat with telencephalic internal structural heterotopias is also a genetic model of epilepsy. The neurons in the heterotopic region lack the radial orientation and laminar pattern. The mutation in these rats results in a wide region of heterotopia under the neocortex, extending from frontal to occipital lobe. These rats show seizure activity after postnatal day 30. Abnormality in cell proliferation and migration is considered to be responsible for this malformation (Lee et al., 1997;Chen et al., 2000;Koplovitz & Skvorak, 1998).

1.2.3 Kindling

The model that will be used in this study is the amygdala-kindling model. It is very good at mimicking partial onset seizures and has been used for over 40 years (Racine, 1972a;Racine et al., 1975;Goddard et al., 1969). We used this model to unveil some pathophysiological aspects of epilepsy, by understanding how kindling supports seizures.

Kindling is a phenomenon in which short daily electrical stimulation of a neuronal site in a limbic region, such as the amygdala or hippocampus, will result in complex partial seizures which then secondarily generalize. In other words, periodical and initially sub convulsive deep brain electrical stimulation of a limbic site will induce both behavioural and electro-graphical changes (after discharge) in the subject animal (Racine, 1972a;Racine, 1972b). Several authors have reported kindling-like phenomenon in human as well (Sato et al., 1990;Coulter et al., 2002). Kindling appears to be the current

model of choice for investigating the functional mechanisms underlying cryptogenic TLE, because of many desirable features. First, kindling is a process which progresses from very first stage of low frequency after discharge (AD) associated with little behavioural response, to the complex convulsive seizure and long AD occurring in stage 5. Racine's staging of kindling process which developed in 1972, clearly classifies the initial movements and head bobbing as stage 1 and 2, mild forelimb clonuses as stage 3 and rearing, loss of balance and falling as stages 4 and 5 (Racine, 1972a). Moreover, as the kindling process passes through further stages, the after discharge threshold or the current intensity threshold to induce focal brain activity decreases significantly, and at the same time the duration of AD considerably increases (McIntyre et al., 2002a). It has also been shown that the epileptic state induced by kindling persists at least one month in the subject animal (McIntyre & Plant, 1993). Furthermore, the kindling process is easily reproducible with relatively no mortality in the animals. Neuropathological studies have shown that in contrast to other animal models of epilepsy, kindling not only causes less neuronal loss, but also reorganizes the neuronal circuitry via synaptogenesis and fibres sprouting (Parent et al., 1998). Numerous studies have identified anatomical, neurochemical and electrophysiological changes that occur due to kindling but the exact mechanism by which kindling induces seizures remains unknown (Bertram, 2007;McIntyre et al., 2002a;Hiyoshi & Wada, 1992;Goddard et al., 1969).

1.3 Piriform cortex

Although once the seizures are induced all limbic regions are involved, our lab has focused on changes that occur in the piriform cortex (PC). The reason for this focus is that it is among the most epileptogenic regions within the limbic region and it has a

relatively simple neuronal structure yet makes an enormous amount of connections to other limbic structures.

The PC is the largest area of the mammalian olfactory cortex, which is characterized by direct input from the olfactory bulb (OB). PC extends over 5 mm of rostral to caudal area in rat forebrain just ventral to the rhinal fissure. PC is located in the paleocortex and is comprised of only three neuronal layers. Layer I contains afferent fibers from the olfactory bulb and few GABAergic horizontal cells. Layer I is further divided to layer Ia which mostly contains afferent fibers from olfactory tract, and a deeper layer Ib containing afferent fibers from other neurons in the PC. Layer II contains afferent fibers from other neurons of PC, superficial pyramidal cells (SP), semi lunar cells (S), and small globular cell (G). Both SP and S cells are glutamergic, but G cells are GABAergic. Layer III has pyramidal and interneuronal cells; however, multipolar cells, which are GABAergic, are the main cell type in this layer (Haberly & Feig, 1983;Haberly & Bower, 1984;Martinez et al., 1987). In addition to major afferent input from lateral olfactory tract (LOT) to the PC, there are some afferent fibers from basal forebrain, the hypothalamus, the thalamus and the brain stem making synaptic connections with PC neurons. There are also vast intrinsic connections between excitatory and inhibitory cells in the different layers of PC. Inhibitory neurons in the PC have been implicated to provide both feed forward (Ballain et al., 1998;Ekstrand et al., 2001;Kanter et al., 1996;Kapur et al., 1997;Princivalle et al., 2000) and feedback inhibition (Ballain et al., 1998;Haberly & Bower, 1984) on pyramidal cells.

Classifying the interneurons based on neurochemical content, for example, the presence of calcium binding protein (CBPs), is one of the useful characterization methods, makes it possible to exactly locate the cells and provides information about the morphology of the interneurons. Calretinin (CR), parvalbumin (PV), and calbindin D28K (CB) are calcium-binding proteins that exclusively expressed in interneurons (GABAergic cells) and not in excitatory (glutamatergic) neurons (McBain & Fisahn, 2001). Recent studies in our lab using CBPs to locate the interneurons in the rat piriform cortex, have shown that the majority (79%) of cell somas of interneurons are in the layer III, while layer II and I of the PC contain only 19% and 1% of interneurons, respectively. This study also indicates that interneurons in PC innervate somata and dendrites positive for the same CBP, with only one exception, which is paravalbumin-calbindin (PV/CB$^+$) interneurons innervating also PV$^+$ dendrites (Gavrilovici et al., 2010a). There are two main inhibitory circuits that connect the inhibitory and excitatory cells in piriform cortex: feed forward and feedback inhibition. To provide feedback inhibition, Layer II pyramidal cells form excitatory synapses on Layer III interneurons. In return, layer III interneurons, which are mostly PV/CB, CB, and PV positive cells, make inhibitory synapses on perisomatic region of Layer II principal cells. In addition, Layer III interneurons with long axons can cross the layers and establish inhibitory synapses on apical dendrites of pyramidal cells (Gavrilovici et al., 2010b;Ekstrand et al., 2001;Suzuki & Bekkers, 2007;Neville & Haberly, 2004). To establish feed forward inhibitory circuit in PC, the afferent axons from mitral cells of olfactory cortex activate the interneurons in layer I. In turn these cells make inhibitory synapses on pyramidal cells in layer II of the PC. The dendrites in layer I of the PC mostly arise from interneurons positive for CB, CR and PV/

CB, with their somata located in layer II and I (Ballain et al., 1998;Ekstrand et al., 2001;Princivalle et al., 2000).

1.3.1 Role of PC in kindling model of TLE

Piriform cortex is part of the limbic system and in addition to its primary role in olfactory perception and memory processing, PC has been widely known as a highly epileptogenic region during kindling. Recent studies have shown that PC has many characteristics, which makes it a good candidate for epilepsy propagation studies. It is possible to kindle PC with the smallest number of stimulations, in contrast to other limbic sites such as hippocampus, which requires many more pulses. This can be because of strong connection between PC and motor cortex (Bolwing et al., 1992). Interictal spikes, which are common features in many epileptic disorders, have been recorded in PC very early in the kindling process, regardless of which limbic site had been kindled. The order of activity of interictal spikes recorded from different brain sites is as follows: PC, amygdala, etorhinal cortex, ventral hippocampus and septal area, while the dorsal hippocampus has not shown any interictal activity. This raises the possibility of PC being one of the main generators of interictal spikes (Kairiss et al., 1984;Racine et al., 1988). In addition, large after discharges can be observed in ipsilateral PC, during early electrical stimulation of other limbic sites (Ebert et al., 1995;Loscher & Ebert, 1996a). Thus, PC could play an important role providing the driving force in the generation of epileptic after discharges. Autoradiographic studies using radiolabeled 2-DG (deoxyglucose) method for investigation of cerebral metabolism and blood flow also showed the early increased activity in the PC after kindling the ipsilateral amygdala (Engel et al., 1978). Also PC is the first region that exhibits induction of immediate-early genes, e.g., c-fos

during the kindling process regardless of kindling site. The expression of c-fos proto-oncogene has been widely used as a marker of neuronal activation during electrical stimulation and can provide insight into the anatomical regions that are activated during seizurogenic process. Induction of c-fos gene and other proto-oncogens such as c-jun, jun-B, jun-D is considered as the first step of alternating effects of electrical stimulation in changing the pattern of neuropeptides and proteins (Loscher & Ebert, 1996a;Morgan & Curran, 1991). Furthermore, it has been shown that while unilateral lesion in the PC can increase the threshold of seizure induction during kindling, bilateral lesion of PC can result in complete blockage of seizure induction upon kindling from the hippocampus or the olfactory bulb. This indicates the crucial role of PC in regulating the excitability in amygdala (Loscher & Ebert, 1996a). Applying GABA-receptor potentiators in the PC can markedly increase the threshold of seizure induction upon kindling from basolateral amygdala (BLA), supporting the idea that the PC plays the major role in seizure propagation (Piredda & Gale, 1985;Piredda et al., 1985).

1.4 Neuronal Network

Diverse populations of cells in the cortex are responsible for processing, transferring and storing the information as distributed networks. Thus, there should be functional mechanisms that can relate the information processed in different assemblies of cells. One possible mechanism is oscillatory synchrony. Neuronal networks in mammalian cortex have demonstrated wide range of oscillatory activity from 0.05 Hz to 500 Hz. Oscillatory activities are the result of interaction between intrinsic cellular and circuit properties (Steriade, 2001;Whittington & Traub, 2003;Traub et al., 1999). Neuronal network oscillations at distinct frequencies have been proposed to play a significant role

in the function of different brain sites. Different frequency classes of oscillations and their correspondent behavioural applications have been preserved throughout mammalian evolution, indicating their major role in different brain sizes (Destexhe & Sejnowski, 2003;Gray et al., 1989;Kahana et al., 2001;Laurent, 2002). Brains oscillators have many functions. For instance, different assemblies of cells can be coupled through oscillations with similar frequencies (Strogatz et al., 1992;Buzsaki et al., 2004). Oscillation can also affect input selection and plasticity of cells (Whittington & Traub, 2003;Thomson, 2003).

Recent studies have shown that the firing of mitral and tufted cells in the olfactory bulb and pyramidal cells in the PC is regulated by two main types of oscillations as gamma (30-80 Hz) and beta (10-30 Hz) (Eeckman & Freeman, 1990;Kashiwadani et al., 1999). Gamma oscillation has been described to originate in the OB and then transfers thorough PC (Becker & Freeman, 1968). Beta oscillation is generated in the OB, PC, etorhinal cortex and dentate gyrus and is more obvious in the PC than OB. Beta oscillation can be generated in olfactory bulb by stimulation with certain organic solvents (Chapman et al., 1998;Zibrowski & Vanderwolf, 1997). In the PC, beta oscillations have been known to play a role in odour sampling and memory (Martin et al., 2007). In the hippocampus, different studies have shown that network oscillations such as theta and sharp-wave-associated ripples are important in encoding, consolidation and retrieval of information (Fox, 1989;Ylinen et al., 1995a;Ylinen et al., 1995b;Csicsvari et al., 1999;Buzsaki, 2002).

Different methods have been used to investigate the oscillatory activity and network characteristics of neurons in the cortex. Local field potentials (LFPs) recording is one of

the methods that has been used for decades to study extracellular electrical activity. In this method, a low impedance microelectrode is placed in the extracellular region of the tissue and measures the electrical potential difference between the microelectrode and the reference electrode (Buzsaki & Traub, 2008). The signal is then low-pass filtered to exclude any individual spike; thus the result is the sum of synaptic input and not the local spiking activity (Mitzdorf, 1985). LFPs recording data can be interpreted by using current source density analysis in which the voltage fluctuation in a given field will be converted to current flows inward or outward the field. LFPs recording coupled with single-cell recording in the hippocampus have shown that diverse interneuron populations have their distinct contributions to neuronal synchrony. Each group of interneurons has distinct firing pattern, and innervate a specific part of pyramidal cells, so they are thought to temporally coordinate firing of pyramidal cells and control the oscillation synchrony, which is necessary for different states of functioning brain (Buzsaki & Chrobak, 1995;Klausberger et al., 2003). LFPs and extracellular single-unit activity were recorded from PC layers II/III also provided some evidence of neuronal synchrony in gamma and beta oscillations (Litaudon et al., 2008;Becker & Freeman, 1968;Freeman, 1978).

Although LFPs recording has provided valuable information on neuronal network oscillations, it has also some limitations. First, we should consider that the excitatory input on the apical dendrite and the inhibitory input on the cell soma both will contribute to the similar effect on the field potential. Because of the identical direction of current flow in these two inputs, the EPSPs and IPSPs will be added. Thus, one cannot distinguish between IPSPs and EPSPs with the use of LFPs recording (Buzsaki & Traub,

2008). The second problem with the LFPs data is the contribution of other factors rather than only EPSPs and IPSPs to the voltage change recorded by this tool. One of the major non-synaptic events is the calcium spike in the dendrites. Such calcium mediated action potentials are generated to boost the synaptic inputs and usually do not travel to the soma (Magee & Johnston, 1997;Markram et al., 1997;Wong et al., 1979). The other non-synaptic event is the intrinsic oscillatory activity of the cell membrane. This voltage-dependent slow oscillatory fluctuation has been recorded from different brain sites such as hippocampus, thalamocortical neurons and stellate cells of etorhinal cortex (Leung & Yim, 1991;Pedroarena & Llinas, 1997). Because the intrinsic oscillatory activity can occur simultaneously in many cells in a local field, they can contribute to a large effect in the LFPs recordings (Haas & Jefferys, 1984;Taylor & Dudek, 1984). It has been also shown that membrane hyperpolarization followed by Ca^{2+} spike usually makes large amplitude changes in the field potential recordings. Calcium-mediated increase of potassium conductance is responsible for this effect (Hotson & Prince, 1980;Schwartzkroin & Stafstrom, 1980). Thus, because of all these factors, LFPs recording is not a perfect tool for recording the oscillatory activity of neuronal networks.

Another valuable technique in studying the neuronal network in the brain cortex is dual whole-cell recording. Using this method Ren et al. (2007), has shown that stimulating a pyramidal cell in layer II/III of the mouse visual cortex can elicit a fast inhibitory postsynaptic current in a nearby pyramidal cell, suggesting that the pyramidal cell is directly innervating the interneurons, which then inhibit the soma of another pyramidal cell (Ren et al., 2007). Another experiment done by Cobb et al. (1995), using dual intracellular recordings has shown that 1-8 Hz stimulus activating basket cells and

axo-axonic interneurons in CA1 region of hippocampus can synchronize the firing of pyramidal cells, which are simultaneously recorded. They also showed that interneurons are able to entrain the pyramidal cells both in sub and suprathreshold level of activity. This study indicated that the combined effects of hyperpolarizing events from interneurons and intrinsic oscillatory level in pyramidal cells will contribute to phase lock activity in theta frequency in principal cells (Cobb et al., 1995).

Although paired and multi-electrode patch clamp recording provide valuable information about the morphology and electrophysiological characteristics of individual cell or basic circuits in the cortex, these techniques have significant limitations regarding the study of neuronal population activity in different layers or columns of the cortex. To overcome this problem, a variety of electrical and optical methods have been introduced (Callaway & Yuste, 2002;Frostig et al., 2008;Schubert et al., 2007). One of these techniques that provides the opportunity for multi-site stimulation and recording is multi-electrode array (MEA). Since the introduction of MEA chips by Thomas et al. (1972) and Gross et al. (1977), they were mostly used to study the network activity in cultured cells and rarely in acute brain slices (Jimbo et al., 2000;Otto et al., 2003;Kopanitsa et al., 2006;Mann et al., 2005;Wirth & Luscher, 2004). This is because of technical problems in making tight seals between the surface of cells in the slices and the microelectrodes. However, cultured cells have enough time to make the necessary connection with the electrodes (Heuschkel et al., 2002). Using micro-electrode-array chips in rat brain slices Bakker et al. (2009), recorded the field potential activity of microcircuits in rat somatosensory cortex. They showed high level of repeatability in spatial pattern of stimulus propagation after stimulation of supragranular, granular and infragranular

layers. They also showed that stimulus response distributes from one column to adjacent columns and the profile of response is different in neighbouring columns (Bakker et al., 2009). Studying the mechanism of network oscillation requires following the population activity in different sites of the brain. Using a combination of multi-electrode array recording, voltage-sensitive dye imaging and single cell recording, Mann O.E et al (1995), tried to unveil the mechanism underlying the gamma generation in CA1-CA3 area of hippocampus in rat brain slices. The results of this experiment indicated the stratum pyramidal as the source of gamma oscillation in CA3 region. However, this oscillation is the result of rhythmic perisomatic inhibitory input to the pyramidal cells. In addition, this study revealed the significant role of feedback input of pyramidal cells on GABAergic interneurons via AMPA receptors. The feedback effect of pyramidal cells synchronizes interneuron firing (Mann et al., 2005).

1.5 Voltage-sensitive dye imaging

Despite the fact that classical electrophysiological techniques have provided vast insights into the mechanism of single cell activity and neuronal circuit synchronization, there are limitations associated with these techniques. For instance, following membrane potential changes in small cells and also in tiny processes of a cell is not feasible by intracellular recording methods. More importantly, the classical field potential recordings using either single or multiple electrodes cannot provide high spatiotemporal information on neuronal population activity. Optical imaging using voltage sensitive dyes (VSDs) seems to be capable of compensating for these limitations. Since its introduction in late twentieth century, voltage-sensitive dye imaging (VSDI) has been accepted as a valuable tool to investigate neuronal activity (Hill & Keynes, 1949;Cohen et al., 1968). VSD

18

imaging is a non-invasive technique, which provides high spatial resolution at the single cell level as well as high temporal resolution in the microseconds range. Using VSD recording it is possible to record the inhibitory changes in membrane potential, while field potential recording technique cannot recognize the inhibitory post synaptic potentials (IPSPs) in the subject cell. On the other hand, VSD imaging can provide valuable information about neuronal circuitry by recording simultaneously from multiple sites. These unique qualities of VSD imaging resulted in development of this technique in recent decades and emerging different kinds of dyes and recording cameras to this field. Voltage sensitive dyes are molecular probes that can transfer the events in membrane potential to the change in optical signal. There are two major categories of voltage sensitive dyes: fast and slow (Waggoner, 1979).

1.5.1 Slow voltage sensitive dyes

Slow dyes, which are also known as "Nernstian" dyes, are membrane permeable and their distribution into the cell follows the Nernst equation (Gross & Loew, 1989). Redistribution mechanism of slow dyes is potential-dependent (Waggoner, 1979;Waggoner, 1988;Chen, 1988;Freedman & Novak, 1989). As the permeability of the dye increases the response time becomes faster. Some examples of slow dyes are positively charged cyanine dyes and negatively charged oxonol dyes (Waggoner, 1979;Chen, 1988;Freedman & Novak, 1989). For example, hyper polarization in the cell membrane results in redistribution of dithiodicarbocyanine dye, diS-C3 − (5), into the cell. Since the dye bound to the cell organelles emits less fluorescence, hyper polarization will result in a reduced fluorescence activity (Sims et al., 1974;Tsien & Hladky, 1978). Slow dyes have been used to map the seizure pathway in rat brain in vivo (Dasheiff,

1989;Sacks & Dasheiff, 1992). Voltage sensitivity of slow dyes is about 1-2% per millivolt change in membrane potential. Although many scientists have used slow dyes to study the membrane potentials in small cells and organelles, this technique has many limitations. One problem is that some other non-Nernstan factors such as dye aggregation inside the cell can result in change in fluorescence intensity, so there is no universal calibration curve for the slow dyes (Reers et al., 1991;Smiley et al., 1991). In addition, the time constant of slow dyes is 1-20 s; therefore these dyes are not suitable for recording fast changes in membrane potential.

1.5.2 Fast voltage sensitive dyes

The second group of optical probes is fast voltage sensitive dyes. These dyes took a lot of attention as a good tool to investigate fast synaptic activity in central nervous system. Fast dyes are amphipathic molecules with the ability to change the emitted fluorescence in according to any alternation in membrane potential (Cohen et al., 1974;Ross et al., 1977;Gupta et al., 1981;Chien & Pine, 1991). Fast dyes respond to the change in the membrane potential in a millisecond time range, thus they can be applied for following the fast synaptic activity. There are four major classes of fast voltage sensitive dyes: (1) merocyanine-oxazolone, (2) merocyanine-rhodanine, (3) oxonol and (4) styryl (aminostyryl pyridinium) dyes (Cohen et al., 1974;Ross et al., 1977;Gupta et al., 1981;Loew & Simpson, 1981).

Different mechanisms have been proposed underlying the fluorescent change of voltage-sensitive dyes in the electrical field. The most accepted mechanisms are molecular motion and electron motion (charge shift mechanism) (Waggoner & Grinvald,

1977;Cohen & Salzberg, 1978;Gross & Loew, 1989). It is obvious that the mechanism responsible for voltage sensitivity in each group of fast dyes is different from the others and depends on the charge and the structure of the dye molecule. Merocyanine dyes have been shown to work based on a rotation-dimer hypothesis, in which any change in the local electric field will result in a shift in equilibrium between monomeric dye molecules oriented perpendicular to the membrane and dimeric dye oriented parallel to the membrane (Ross et al., 1974;Ross et al., 1977). Other studies suggested that the mechanism underlying the action of negatively charged axonol dyes, WW781 and RGA 461, is an on-off mechanism by shifting the chromophor between the membrane surface and locations within the membrane which subsequently changes the emitted fluorescent spectra (George et al., 1988).

Of more interest are Styryl probes such as di-5-ASP and di-4-ANEPPS, which have been extensively studied and synthesized by Loew and colleagues (Loew et al., 1979;Loew et al., 1985;Loew & Simpson, 1981;Fluhler et al., 1985). The structure of styryl probes is consisted of a quarterized pyridinium linked to amino phenyl via one or double bounds (Cohen et al., 1974;Ross et al., 1977;Gupta et al., 1981). The voltage sensitive properties of styryl dyes can be explained by electrochromism mechanism. Electrochromism is a phenomenon displayed by some materials in which any change in electrical field shifts the absorption peak frequency of the material, therefore results in changing color (Waggoner & Grinvald, 1977;Loew & Simpson, 1981;Gross & Loew, 1989). After binding to the membrane, the positively charged pyridinium ring is oriented toward the extracellular space, keeps the long axis of the probe perpendicular to the membrane surface. Excitation in the electrical field shifts the positive charge from

pyridinium ring to the amino phenyl end of the molecule. Thus, relocation of the positive charge alters the fluorescent emission frequency and produces the blue shift of the spectrum for these dyes (Loew et al., 1978;Loew et al., 1979). Styryl dyes are not fluorescent in aqueous solution and also they show different spectral properties based on their environment (Montana et al., 1989). During last decades, about 1800 voltage sensitive dyes have been tested but less than 200 of them have displayed enough sensitivity to follow membrane voltage change with minimum toxicity (Cohen et al., 1974;Ross et al., 1977;Gupta et al., 1981). Di-4-ANEPPS (4 represents the number of carbons in each of the alkyl chains, aminonaphthylethylene pyridinium propylsulfonate) is one of the best fast dyes applied for optical recordings. This dye shows a change in fluorescent of 8-10% for 100mV change in membrane potential. This is not the ideal voltage sensitivity for the fast dyes while the dye RH421 shows 21% change on neuroblastoma cell preparation (Grinvald & Farber, 1981;Grinvald et al., 1983). However, di-4-ANEPPS has shown a considerably consistent response in different preparations, which is not the case for dye RH421. The fluorescence response of di-4-ANEPPS has been consistent in numbers of cultured cell lines, red blood cells and bilayer model membrane (Gross et al., 1986;Fluhler et al., 1985). The maximum fluorescence excitation/emission spectra of di-4-ANEPPS bound to neuronal membranes are ~ 475/617 nm. Hyperpolarization in the cell membrane results in a decrease in fluorescence excited at approximately 440 nm and an increase in fluorescence excited at 530 nm (Montana et al., 1989). Di-4-ANEPPS has no net charge at neutral pH. It also causes less photodynamic damage than other voltage sensitive probes (Fromherz & Vetter, 1992). Di-4-ANEPPS is the dye we used in our experiments.
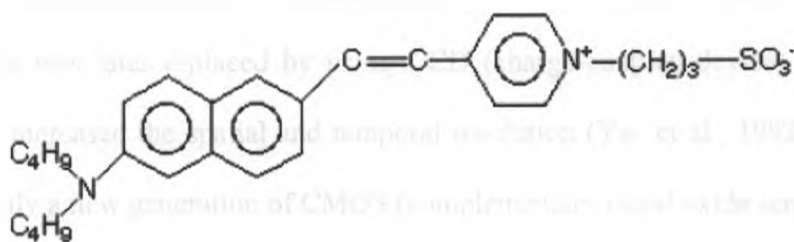
Figure 1- Di-4-ANEPPS

[1-(3-sulfonatopropyl)-4-[beta- [2-(di-n-butylamino)-6-naphthyl] vinyl] pyridinium betaine]

1.5.3 Optical recording methods

Since the optical signals produced by voltage sensitive dyes are small in size, it is important to utilize a powerful imaging system. Two major optical recording systems are photodiodes and video imaging. A photo-iodide detector is capable of converting light to current or voltage. Any photon with enough energy can excite an electron in this system making a free electron. Single photon multiplier tubes and single photodiodes, were the first methods used to detect the optical signal. However, due to their limited spatial resolution these techniques were mostly replaced by multiple photodiodes and photodiode arrays (Tasaki et al., 1968;Cohen et al., 1974;Ross et al., 1974;Salzberg et al., 1977;Grinvald et al., 1977;Grinvald et al., 1981).

The other optical recording technique is video imaging. Loew and colleagues were the first to introduce the application of video imaging in recording the voltage-sensitive dye signal. They used this method to map the spatial propagation of externally applied

transmembrane potential changes in non-excitable cells (Gross et al., 1986). Conventional tube technology was initially applied for VSD video imaging. However, this technique was later replaced by using CCD (charge-coupled device) camera that considerably increased the spatial and temporal resolution (Yae et al., 1992;Elias et al., 1993). Recently a new generation of CMOS (complementary metal oxide semiconductor) based cameras, have increased even more the temporal and spatial resolution in VSD imaging. CMOS based cameras have the temporal resolution of about 10,000 frames/second and a quantum efficiency of 60%. They also provide a spatial resolution of 100 x 100 pixels, covering an area of 10 mm x 10 mm in the slice (Lieke et al., 1989;Ts'o et al., 1990)

One of the most important parts of VSD recording set-up is the light source used to excite the dye. Since the optical signal of the dye in CNS preparations is at a fraction of 1% relative to background fluorescence, we need a stable light source. Furthermore, the light source should be sufficient to excite the probe. Depth of the recording is the other factor that considerably affects the light intensity. In epi-fluorescence recording both the illuminating light and the emission light are fall-off by a factor of 10/mm, resulting in a reduction of signal to noise ratio of 10/mm (Orbach & Cohen, 1983). Two major classes of light sources used in VSD imaging set up are tungsten-halogen lamps and mercury arc lamps (Grinvald et al., 1981). Mercury arc lamps produce high intensity illumination at wide spectral ranges, such as 546.1 nm that is suitable for exciting the RH414 and di-4-ANEPPS. However, the mercury arc lamps are unstable and possess both the fast and slow noise (Chien & Pine, 1991;Orbach & Cohen, 1983). On the other hand, the halogen lamps have the advantage of more stability over arc lamps (Kamino et al., 1989).

1.5.4 Optical signal analysis

Measurements of optical signal are usually done by reporting the change in the fluorescence (ΔF) as a fraction of the background level ($\Delta F/F$). Different factors such as dye, lens and tissue characteristics can affect the intensity of the recorded signal. Dyes with greater difference in fluorescence level between two states (ground and excited states) will show stronger change in optical signal. To obtain better fluorescent signal it is also necessary to use a lens with high numerical aperture. In addition, one of the factors that considerably decreases the optical signal is the unspecific binding of the dye (Waggoner & Grinvald, 1977). The change in light intensity depends on the membrane area and changes in membrane potential. Thus, elements with high surface to volume ratio, will contribute greater to the recorded signal. This includes dendrites, axons and also the glial cells (Grinvald et al., 1983;Bonhoeffer & Staiger, 1988;Loew et al., 1992). Loew et al. (1985) showed that the fluorescence change in squid axon stained with di-6-ASPPS is 20-40 folds lower than stained hemispherical bilayers. This is because of high level of background fluorescence emitted from non-specific staining (Loew et al., 1985). Although it is possible to increase the signal by increasing the light intensity, this can result in phototoxicity. It has been shown that dye molecules in the presence of illumination can form reactive oxygen and other free radicals. These reactive components can damage the cell (Pooler, 1972;Cohen et al., 1974;Ross et al., 1977). The other issue is dye internalization, which reduces the signal. However, new improvements in dye structure such as reduced internalization and phototoxicity in combination with using fast CCD based cameras which need less light to record the activity has contributed to

increased imaging quality. It also provides the opportunity to record the tissue activity for hours without any change in physiology (Obaid et al., 2004;Ang et al., 2005).

Voltage-sensitive dye imaging has been used in wide range of preparations from recording the electrical activity of tiny processes of cultured cells (Grinvald et al., 1983;Grinvald et al., 1981) to mapping the activity of the mammalian cortex *in vivo* (Woolsey & Van der Loos, 1970;Orbach & Cohen, 1983;Kobayashi et al., 2010;Biella et al., 2010;Petersen et al., 2003;Cinelli & Kauer, 1995). VSD imaging has also been applied to study the synaptic response in the synaptic site by injecting the VSD into a single cell (Cohen et al., 1974;Gupta et al., 1981). To demonstrate the validity of VSD imaging in following the changes in membrane voltage, some set of experiments have been done. In these experiments scientists tried to calibrate the data of VSD imaging by combing it with other techniques such as whole cell patch clamp and local field potentials recordings. Using dye di-4-ANEPPS, Tominaga et al. (2000), showed that the trace of voltage membrane change obtained by optical recording follows the same pattern as intracellular recording and field potential recordings, suggesting that the optical signal essentially measures the change in membrane potential of postsynaptic neurons. They also demonstrated that the optical signal of di-4-ANEPPS dye recorded by the MiCAM ULTIMA camera (the same setup we are using in our experiments) is relatively stable without making any perturbance in cell physiology (Tominaga et al., 2000). Other investigators have also demonstrated the linear relationship between fluorescence change and the change in membrane voltage recorded by current clamp techniques. This relationship was over a physiologic scale of (-5 to +30 ΔVm) of about 0.1% ΔF/F for each 10 mV voltage change for JPW 3031 dye (Carlson & Coulter, 2008). Hippocampus

is one of the brain regions has been widely studied by VSD imaging. Because of laminar structure of hippocampus circuitry and distinct afferent and efferent projections, it is ideally suited for VSD imaging. VSD imaging has been used to study the physiology and signal propagation in hippocampus (Grinvald et al., 1982;Saggau et al., 1986;Bonhoeffer & Staiger, 1988;Bonhoeffer et al., 1989). By stimulating the alveus the resulting antidromic activation of CA1 pyramidal cells generates optical signals consistent with hyperpolarization in the CA1 region of the hippocampus in rat brain slices (Grinvald et al., 1982;Carlson & Coulter, 2008;Tominaga et al., 2009). Since IPSPs are really sensitive to both internal anion concentrations that are usually disturbed in whole- cell recordings and holding current, it is not possible to follow the inhibitory activity accurately by patch clamp methods. Thus, recording the ensemble inhibitory activity of neuronal population is one of novel applications of VSD imaging. On the other hand, VSD imaging is a valuable tool to study seizure propagation because of possibility to record from different regions in the tissue simultaneously. Voltage sensitive probes have been used to study the origin and propagation pathway of interictal activity in hippocampus slices from different species. CA2-CA3 regions have been implicated as the origin of interictal spikes, with some variances in different species (Colom & Saggau, 1994).

Optical imaging of the piriform cortex has also provided some information about the signal propagation in the control state and also after application of different drugs. Electrical stimulus to the layer Ia of piriform cortex resulted in propagating of the signal to the layers II and III, and in some slices to the adjacent endopiriform nucleus. These findings were consistent with the results of field potential recordings done

simultaneously in the same tissue, with the maximum peak of fluorescent signal coincided with the maximum negativity in the field potential recording (Sugitani et al., 1994a;Sugitani et al., 1994b;Demir et al., 1998a). By applying bicuculline methiodide, a $GABA_A$ receptor antagonist, to the bath the fluorescence signal can distribute over a larger area even with a smaller stimulus current (Demir et al., 1998b).

2. Working Hypothesis

Recent evidence in our lab has shown interneurons (INs) within the piriform cortex are more inhibited after kindling (Gavrilovici et al., 2006). On the other hand, we know that INs have both inhibitory connections on pyramidal cells and reciprocal connections with other interneurons (Haberly & Feig, 1983). We also know that layer III contains the highest PC interneuron population (Haberly, 1983;Haberly et al., 1987). Since INs are important for inhibiting the activity of the principal cell layer, this raises the possibility that increased disinhibition may lead to seizures. Thus, the hypothesis that will be investigated here is that **the occurrence of disinhibition in the layer III of piriform cortex provides the driving force for activation of principal cells in layer II and increased level of disinhibition in the PC is responsible for the seizure activity after amygdala kindling.** To test this hypothesis, we first needed to characterize the occurrence of disinhibition in the layer III of PC using voltage-sensitive dye imaging from the slices of control rats. We also investigated the impact of different conditions (stimulus frequency) on the level of disinhibition. In addition, we tested the effect of a pharmacological agent that alters the GABAergic inhibition on piriform cortex. Finally, we addressed the effect of kindling-induced seizures on inhibitory and excitatory activity in the piriform cortex to gain better understanding how kindling can change the disinhibition.

3. Materials and Methods

All experiments were conducted in accordance with the guidelines of the Canadian Council on Animal Care and approved by university of Western Ontario council on animal care.

3.1 Kindling

Rats were divided in two groups. A group of rats were implanted with bipolar electrodes in basolateral amygdala (BLA) for kindling and the second group was control non-kindled rats. Male Sprague Dawley rats weighing 200 g were anaesthetized with 0.1 cc/1000g of a mixture of ketamine and domitor (medetomidine hydrochloride) solution. The stimulating/recording electrodes were implanted in both right and left basolateral amygdala by using stereotactic surgery set-up with the following coordinates: 2.6 mm posterior to Bregma, 4.5 mm lateral to midline and 8.0 mm ventral (Paxinos & Watson, 1986). The electrodes were constructed of two twisted strands of 0.127-mm diameter Diamel-insulated Nichrome wire and were attached to male Amphenol pins. The electrodes were implanted and secured to the skull with jeweller's screws. Dental acrylic cement was used to fix the electrodes in the skull (McIntyre & Molino, 1972). Kindling was started one week after surgery. The after discharge threshold (ADT) was determined in each amygdala by delivering a 2-s 60-Hz sine wave stimulus of progressively increasing intensity (15, 25, 35, 50, 75, 100, 150, 200, 250, 300 and 350 μA) until an after discharge was triggered (McIntyre & Plant, 1993). Daily kindling in one side amygdala was continued until observation of stage 5 seizures according to Racine's

staging in 3 consecutive days (Racine, 1972a). Then the rats were allowed to recover for 2 weeks before slice preparation.

3.2 Slice preparation and staining

In the day of the experiment a rat was deeply anaesthetized with the domitor-ketamine solution, the chest wall was opened then ice-cold choline solution was perfused through the heart. Choline solution contained (in mM) choline Cl, 110; KCl, 2; NaH_2PO_4, 1.2; $NaHCO_3$, 25; $CaCl_2$, 0.5; $MgCl_2$, 7; Na pyruvate, 2.4; ascorbate, 1.3; dextrose, 20 (McIntyre et al., 2002b). Then the rat was decapitated and brain was removed. The temporal lobe area was excised as a block and subsequently sliced coronally with a Vibratome in 400µm-thick sections. The slices were obtained from 2.2 to 0.2 mm relative to bregma. The slices were incubated at 37 °C for 30 min and then moved to a room-temperature (22 °C) bath for at least 45 min. Slicing, incubation and storage were all performed in the choline solution. The ACSF (artificial cerebrospinal fluid) solution that run through the bath during the recording was similar to choline solution except that pyruvate and ascorbate were removed and equimolar NaCl replaced the choline Cl. $MgSO_4$ and $CaCl_2$ were used at concentration of 1 mM in this solution. All solutions were maintained at pH 7.4 and bubbled with 5% CO_2/95% O_2 (carbogen). For staining, the slices were incubated for 30 min in a solution contains 0.6 mM of dye di-4-ANEPPS (D-1199, Invitrogen Molecular Probes Inc., OR, USA); dissolved in ethanol to a stock concentration of 10.4 mM, 500µl of Ringer's solution, 500 µl of fetal bovine serum (FBS) and 19.2 µl of 10% Cremophore-EL solution. After washing the slices for 10 min with choline solution in another well, slices could be transferred to the recording chamber. To minimize the effect of dye on the cells, we used the minimum concentration

of dye. For this purpose, we performed a set of experiments with different concentrations of dye. The final concentration of 0.6 mM was the minimum concentration that provided suitable fluorescence intensity in our preparation. The slices were continuously bubbled with carbogen during the staining process to keep the pH and oxygen concentration constant. In the recording chamber the slices were stimulated with one -second electrical stimulus at the border of lateral olfactory tract (LOT) and layer I of piriform cortex. The stimulation of each slice was started with low current intensity, and then the intensity was gradually increased (16-20 µA) until we could follow the propagation of activity from the electrode tip to the different layers of PC in the recorded movie.

3.3 Optical recording

VSD imaging experiments were conducted in the piriform cortex before and after stimulating LOT with different frequency entrainment. Each recording was 20470 ms lengths and consisted of two parts; the first part was 2000 ms recording of background activity before the stimulus followed by the stimulus application for 1s with frequencies differing from 20-80 Hz. A Platinum/Iridium electrode (MicroProbes, Inc., MD, USA) with the tip diameter of 2-3 µm was used to stimulate the LOT. The electrode was connected to a stimulator (S88X dual output square pulse stimulator, Grass Technologies, An Astro-Med, Inc., QC, Canada), which provided the pulse with different frequency and duration. The slice was submerged on the chamber through which oxygenated 30°C Ringer's solution flowed. Optical recording was conducted using a CMOS camera (Micam Ultima, BrainVision, Inc., Tokyo, Japan) mounted on top of an upright microscope (Fixed Stage Upright Microscope BX51WI, Olympus). The light from a 100W halogen lamp source (HLX 64625, Microlites Scientific, Corp.) passed through an

excitation filter ($\lambda=530 \pm 10$ nm) and reflected by a dichoric mirror illuminated the slice. The fluorescence signals were collected and projected onto the CMOS sensor through an absorption filter ($\lambda > 590$ nm). A long distance lens was used in these experiments (XLFluor 4X/340 NA 0.28, Olympus). The movies were recorded and analyzed using Brain Vision Analyzer (Tokyo, Japan) software. The acquisition settings were: 100×100 pixels frame size, 10 ms sampling time and 25 μm $\times$ 25 μm pixel size. Di-4-ANEPPS dye shows a uniform 1% change in fluorescence per 10 mV change in membrane potential. The fractional change in fluorescence signal relative to background signal ($\Delta F/F$) was calculated for each recording. For all the recordings, we binned 3x3 pixels into one pixel. We used two forms of analysis for our recordings; in one set of our recordings we defined the average of three pixels, as the region of interest (ROI). Each ROI covered an area of 75x75 μm in the slice. To correct the variable fluorescence values among different slices, the percent change in peak fluorescence in each ROI was normalized by the peak amplitude of 20 Hz stimuli from the same ROI. To analyze the effect of different chemicals on cells population activity in layers II and III of piriform cortex stripe analysis was applied. Each stripe consisted of 10 pixels and covered an area of 250 μm lengths. The data driven from each stripe was the average $\Delta F/F\%$ of 10 pixels. The stripes were manually placed on adjacent areas in layers II and III of piriform cortex according to anatomical landmarks (see Figure 2). Because of small size of VSD signal, bleaching can strongly affect the data; therefore we subtracted a non-stimulated area of recording from all other points to correct for bleaching. It is also important to note that in reality, dye signal intensity decreases as membrane depolarizes; however, to better

match conventional recordings, the signals all have been converted so that the excitatory and inhibitory signals were shown as positive and negative values, respectively.
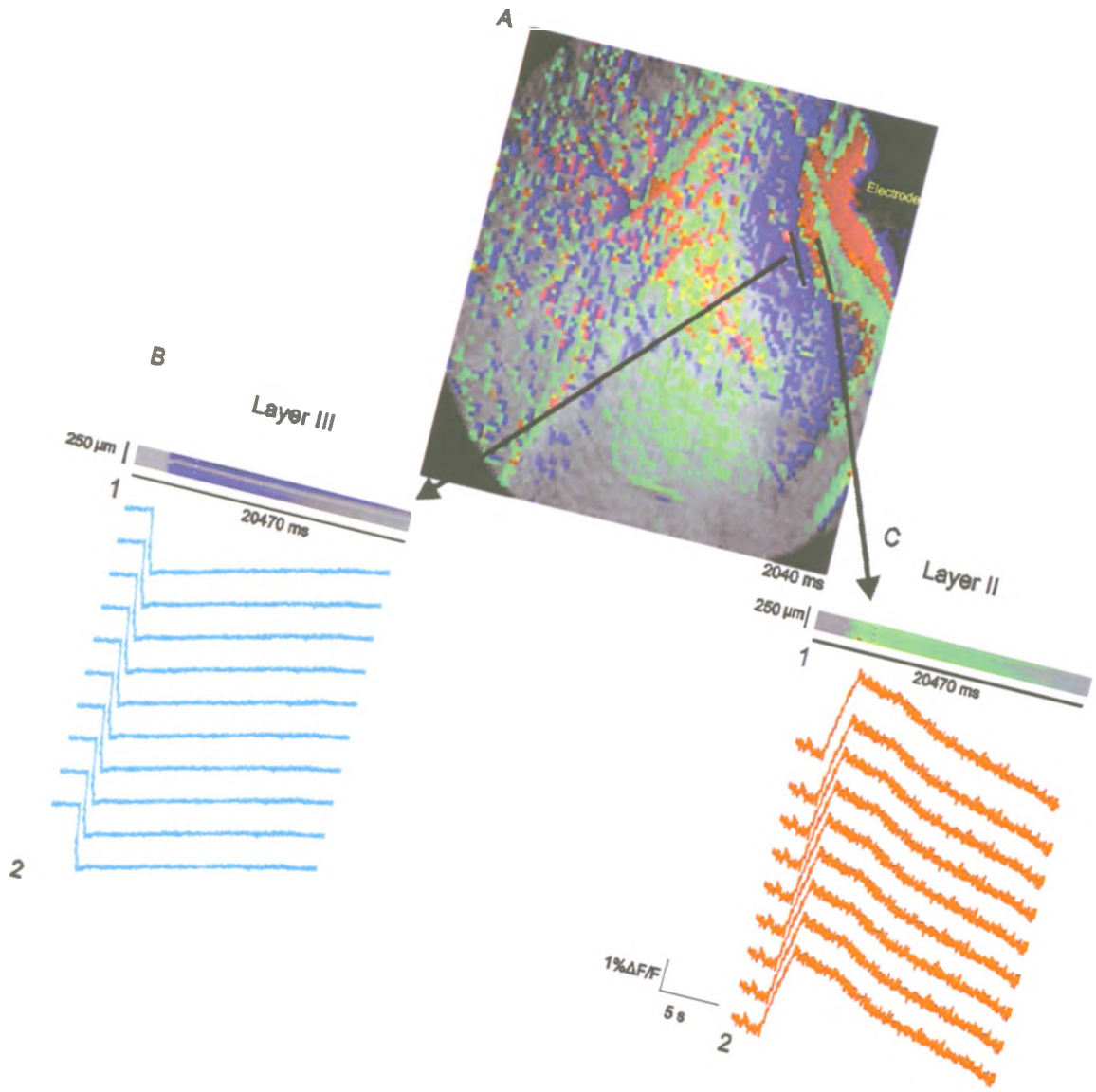
A

Electrode

2040 ms

B

Layer III

250 µm |

1

20470 ms

2

C

Layer II

250 µm|

1

20470 ms

1%ΔF/F|

5 s

2

Figure 2- A stripe was used to calculate the average change in peak fluorescence in a region of interest.

Each stripe covers an area of 10 pixels. (A) A filmstrip demonstrates the neuronal activity in pseudo colours 40 ms after stimulation the LOT with 60 Hz pulse. The stripes are shown as two parallel lines in layers II and III of piriform cortex. (B) A stripe drawn on layer III of piriform cortex is predominately consisted of inhibitory responses. (B1) Illustrates the changes in VSD signal along a line for each time point. (B2) Each wave represents the fluorescent change in a pixel along the stripe. (C) A stripe drawn on the layer II shows mostly the excitatory responses in all the pixels. (C1) Shows the changes in VSD signal along a line for each time point. (C2) Each wave represents the fluorescence change in a pixel along the stripe.

To test whether the VSDI exactly follows the change of voltage in the cell membrane, we performed some experiments before and after running the high-K^+ solution ($[K^+]_0 = 30$ mM) in the bath. Switching from control Ringer's solution ($[K^+]_0 = 3$ mM) to high-K^+ solution should cause depolarization in the membrane potential. The recorded results showed an average decrease of about 4% in fluorescence signal that corresponds to a 30 mv depolarization in the membrane potential (1% $\Delta F/F = 7$ mv). This agrees with predicted depolarization calculated from the Nernst equation (n= 4 slices from 2 rats, p = 0.007 paired t-test, Figure 3).

We also attempted to test if the changes in the fluorescence signal during VSDI were caused by action potentials from postsynaptic activities. For this purpose, VSDI of rat piriform cortex was performed before and after applying 1 μM tetrodotoxin (TTX), a sodium channel blocker, in the bath. The results demonstrated a significant reduction in fluorescent activity as the peak amplitude of fluorescence signal disappeared within recordings 10 minutes after applying TTX. Therefore, we concluded that the postsynaptic activity is the underlying cause of changes in fluorescence signal.
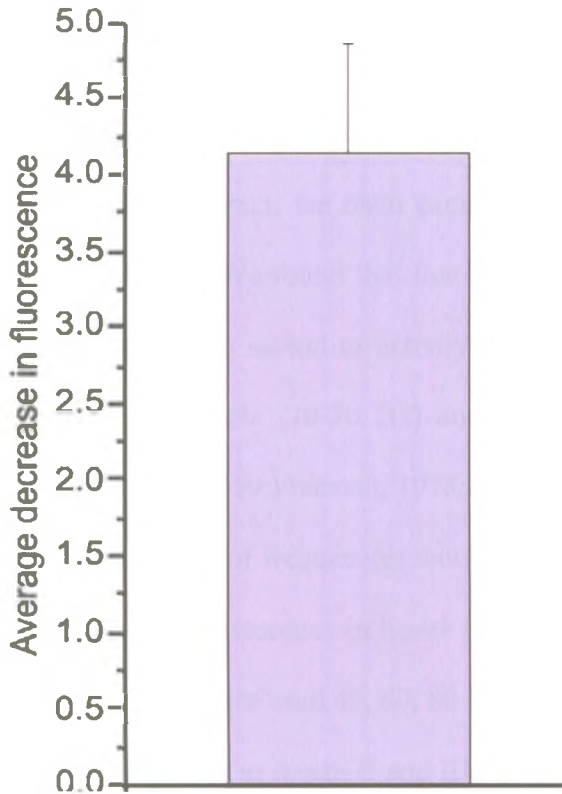
Figure 3- High-K$^+$ solution decreases the fluorescence intensity.

Fluorescence intensity decreases after incubating the slices in high-K$^+$ solution ([K$^+$]$_0$ = 30 mM for 15 min]. The decreased fluorescence intensity indicates cellular membrane depolarization (n= 4 slices from 2 rats).

4. **Results**

We were interested to find out how the piriform cortex responds to electrical stimuli of the olfactory tract, the main excitatory input to the layer I dendrites of the layer II pyramidal cells. We found that low frequency and single stimuli were not sufficient to elicit a significant spread of activity within the slice. As olfactory bulb output is often occured in the beta (10-30 Hz) and gamma (30-80 Hz) bands of activity (Bressler, 1984;Freeman, 1959;Freeman, 1978;Kay & Freeman, 1998), we decided to see if stimuli over these bands of frequencies would induce significant network activity. We recorded the change in fluorescence in layers II and III of PC before and after stimulating the slice with 10, 20 Hz (beta) and 40, 60, 80 Hz (gamma) stimuli. Two regions of interest in each slice were chosen in layers II and III of piriform cortex. As outlined in the methods, the percent change in peak fluorescence in the regions of interest (ROI) was normalized by the peak amplitude of 20 Hz stimuli from the same ROI. Responses to 10 Hz stimuli were weak and variable; however, over the range of 20-80 Hz robust responses were observed. We found two kinds of responses, one where the fluorescence intensity decreased (indicating an increase in activity; excitation) and another where the fluorescence increased in intensity (indicating a decrease in activity; inhibition). To better correlate with intracellular recording results, we showed the excitatory response with positive value and the inhibitory response with negative value (Figure 4). These two forms of activities were presented in all of the recorded slices with differences over the size of propagation area. The excitatory responses were mainly seen around the electrode tip up to layer II of piriform cortex (anatomically represents as a dark layer, more populated with cell bodies). In addition, in some of the slices the excitatory responses

were seen in a deeper area after layer III as a circular region of activity separated from its surroundings, which is known as endopiriform nucleus (EN). The inhibitory responses were located mostly in layer III of piriform cortex. As shown in Figures 5 and 6 there was a significant increase in the excitatory responses in the range of 10 Hz to 80 Hz in layer II of piriform cortex (n= 6 slices from 5 rats, p = 0.006 R= 0.993, Figure 6). The inhibitory responses were also enhanced by higher stimulation frequencies in layer III of piriform cortex (n= 5 slices from 4 rats, p = 0.007, R= -0.96, Figure 7). However, the 10 Hz stimuli often produced no inhibitory response. So this level of stimulation was unable to produce significant network activity.

A

0 s	1.7 s	3.4 s	5.1 s
6.8 s	8.5 s	10.2 s	11.9 s
13.6 s	15.3 s	17 s	18.7 s

B

1%ΔF/F

6 s

41
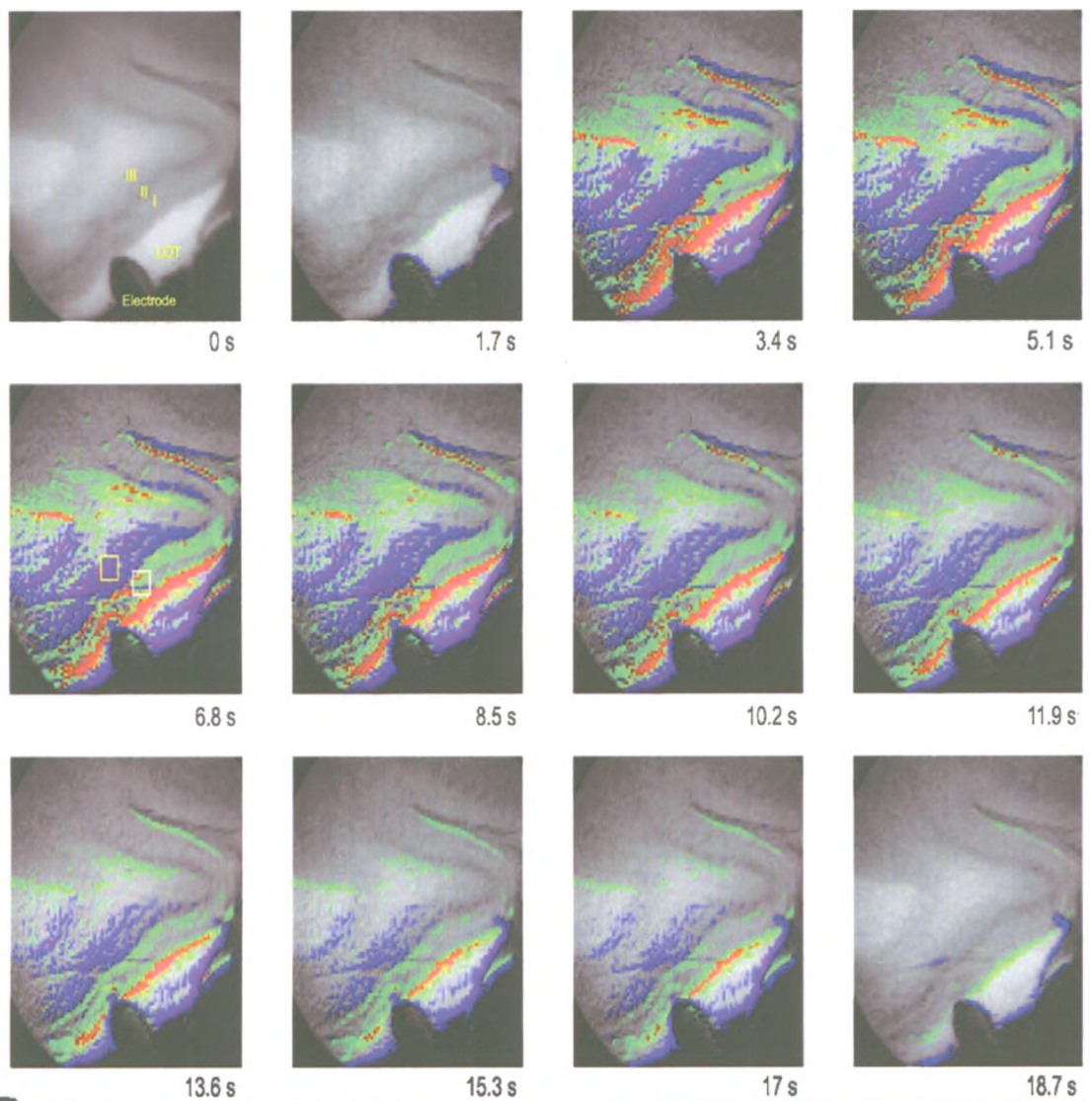
Figure 4- Voltage-sensitive dye imaging (VSDI) of neuronal activity in piriform cortex.

(A) The filmstrip shows propagation of an evoked VSD signal from lateral olfactory tract to three layers of piriform cortex (layers I, II and III). The electrical stimulus was applied to the lateral olfactory tract 2 s after the start of the recording. The pictures are depicted every 1.7 s. Pseudocolours of the images represent excitatory and inhibitory responses to the stimulation. Warmer colors (red) represent excitation while the colder colors (blue) represent inhibition. (B) Responses are shown as waves that are representative of percentage change in fluorescence in two regions of interest. Each square represents a region of interest (ROI) of 3x3 pixels area. The yellow square placed on layer III shows mostly inhibitory responses. The white square on layer II has predominately excitatory responses.
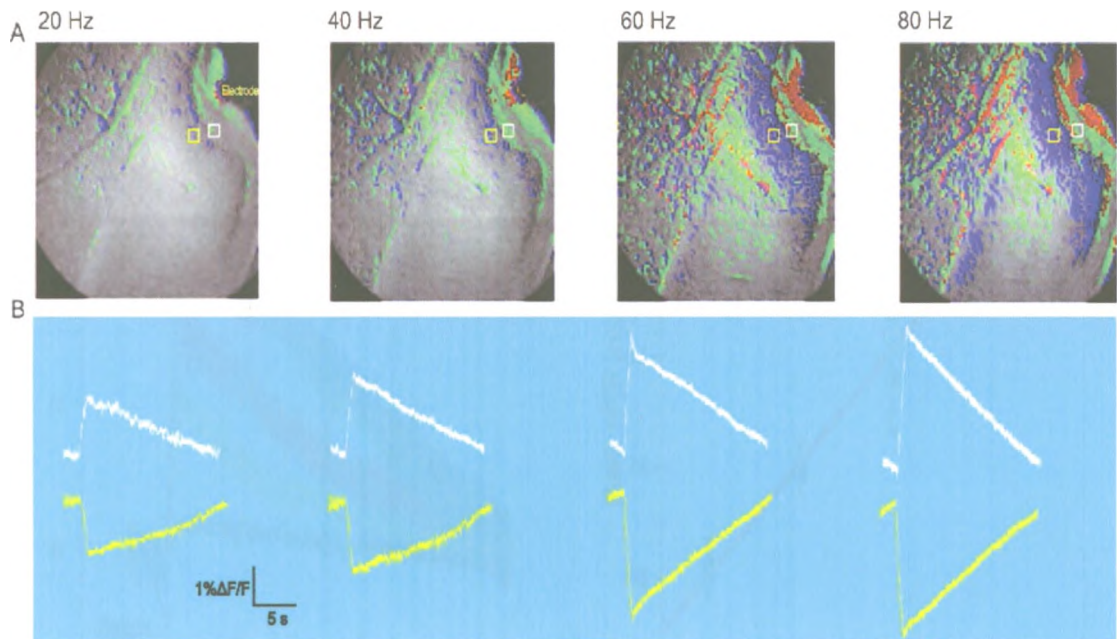
Figure 5- Excitatory and inhibitory responses increase with higher stimulus frequencies.

(A) Filmstrips depict the propagation of neuronal activity in piriform cortex in a single slice after stimulation by different frequencies (20 Hz, 40 Hz, 60 Hz and 80 Hz). They illustrate the fluorescent activity 50 ms after stimulus in 4 recordings from the same slice. Warmer colors (red) represent excitation while the colder colors (blue) represent inhibition. (B) Illustrations of inhibitory and excitatory responses to different stimulus frequencies. Waves demonstrate the percent change in fluorescence in two regions of interest over the time. The white and yellow squares placed on layers II and III of piriform cortex show excitatory and inhibitory responses, respectively.
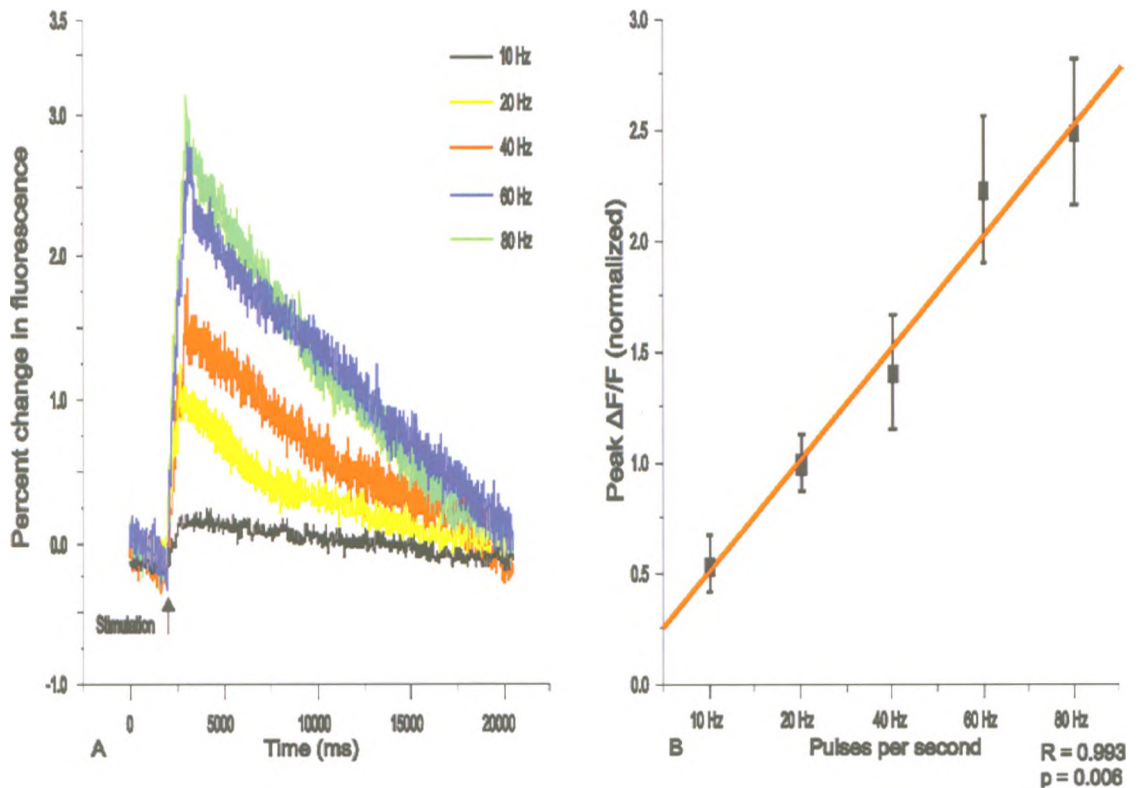
Figure 6- Excitatory response increases linearly over the range of 10-80 Hz in control slices.

(A) One second-long trains at different frequencies show a progressive increase in the excitatory responses. Each wave represents the average change in fluorescence in a ROI placed in layer II of piriform cortex (n= 6 slices from 5 rats). (B) The peak fluorescence amplitude increases in the range of 10-80 pulses per second in a linear manner. The average peak fluorescence for each frequency was normalized by the average peak of 20 Hz recordings. Linear regression analysis was used to fit the line.
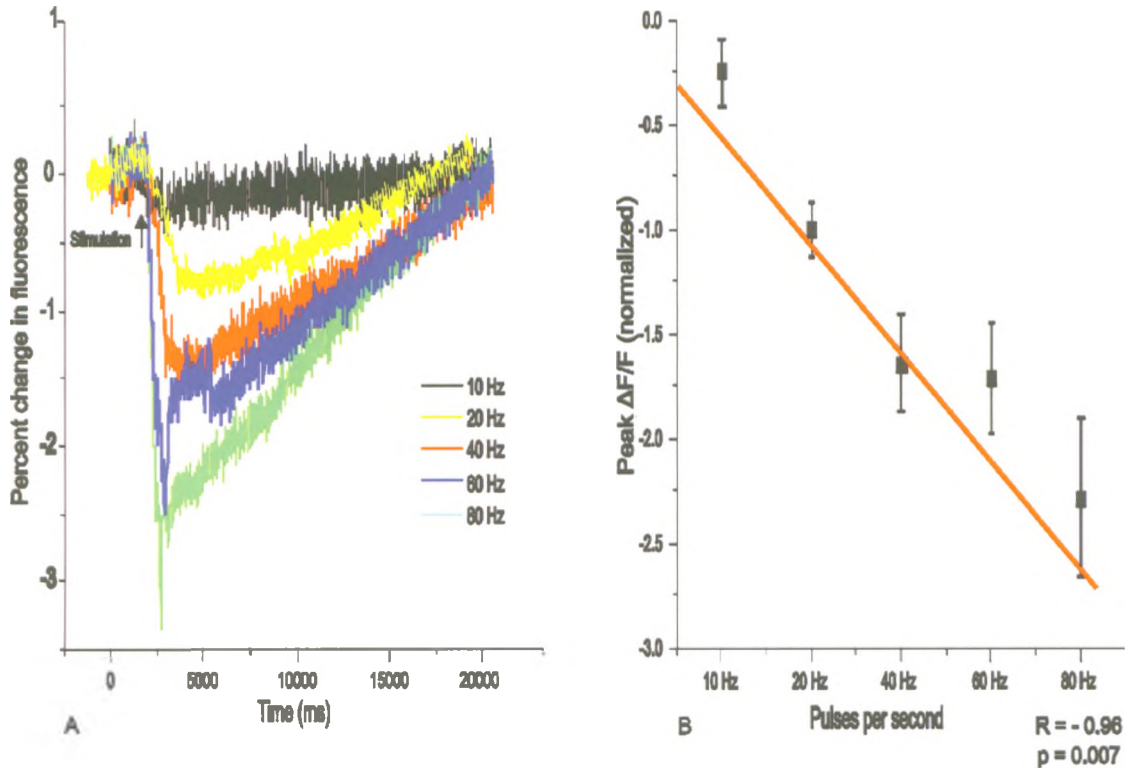
Figure 7- Inhibitory response increases linearly over the range of 10-80 Hz in control slices.

(A) One second-long trains at different frequencies show a progressive increase in the inhibitory responses. Each wave represents the average change in fluorescence in a ROI placed in layer III of piriform cortex (n= 5 slices from 4 rats). (B) The peak fluorescence amplitude increases in the range of 10 to 80 Hz pulses per second in a linear manner. The average peak of fluorescence response for each frequency was normalized by the average peak of 20 Hz stimulus. Linear regression analysis was used to fit the line.

To better clarify the input/output relationship in pirifrom cortex, we tried to find out whether the excitatory and inhibitory responses were sensitive to different frequency entrainment rather than number of pulses. For this purpose, we stimulated the slices by 60 pulses at different frequencies (20, 40, 60 and 80 Hz). As the results show in Figure 8, the excitatory responses were only significantly sensitive to the 60 Hz stimulation (n= 11 slices from 4 rats, p = 0.03). The inhibitory responses, however, were not sensitive to different stimulus frequencies (n= 6 slices from 4 rats, p > 0.05).

Since the evoked response spreads from the LOT to different layers of the PC, we calculated the timing when the evoked response reached layers II and III of pirifrom cortex. The results showed that the excitatory response in layer II preceded the inhibitory response in layer III. Furthermore, the lag time between inhibitory and excitatory responses decreased significantly with higher rates of stimuli (n= 12 slices from 7 rats, p = 0.03, Figure 9). To better understand the effect of higher frequencies of stimulus on the timing of excitatory and inhibitory responses, we next measured the rate of change of excitatory and inhibitory fluorescence responses after stimulation. For this purpose, we chose two regions of interest (ROI) of 3x3 pixels size in layers II and III of piriform cortex, then we divided the peak fluorescence amplitude of each wave by 10-90% rising time of the same wave. The results indicated an increase in response rate of both excitatory and inhibitory activities with higher stimulus frequencies in the range of 20-80 Hz (The excitatory response: n= 13 slices from 7 rats; inhibitory response: n= 10 slices from 7 rats, Figure 10).
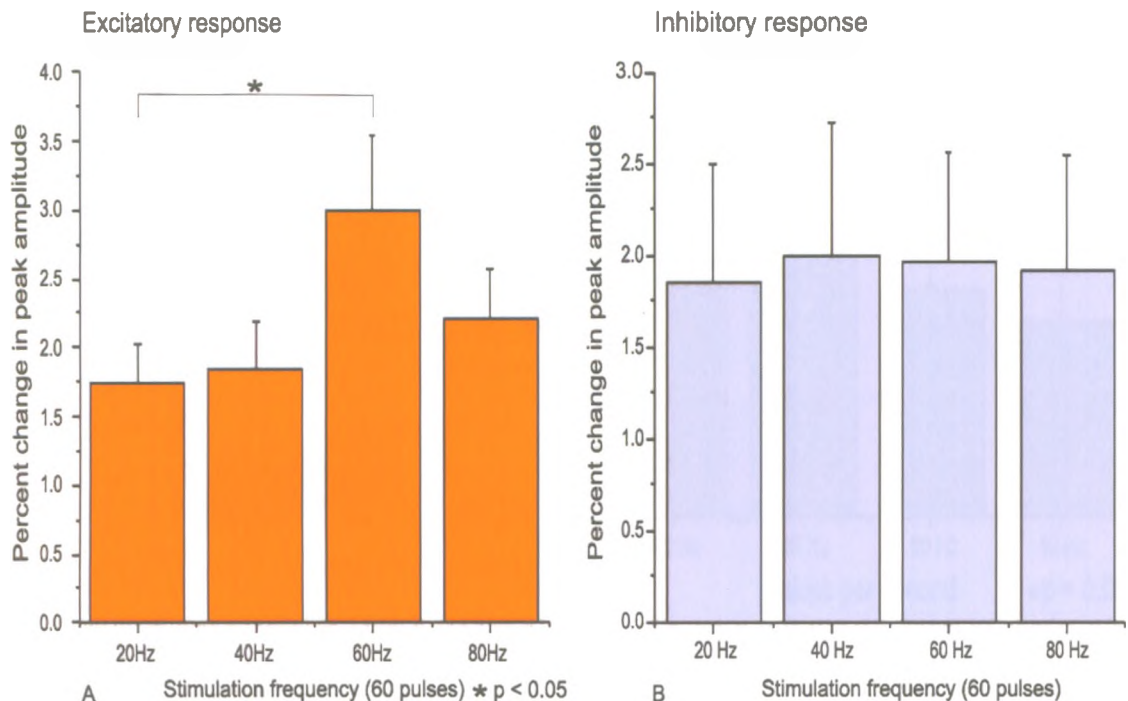
Figure 8- Differential sensitivity to frequency between excitatory and inhibitory responses in control slices.

To test if responses are sensitive to different stimulus frequencies, 60 pulses were applied to the slices at different frequencies. A 10 pixel-stripe was used to calculate the average change in peak fluorescence in each recording. All data were normalized by the peak of 20 Hz stripes. (A) Excitatory responses were sensitive to increased stimulus frequency from 20 Hz to 60 Hz (n= 11 slices from 4 rats). (B) Inhibitory responses were not sensitive to stimulus frequency (n= 6 slices from 4 rats). The statistical analysis was done using one-way ANOVA followed by Post hoc analysis.
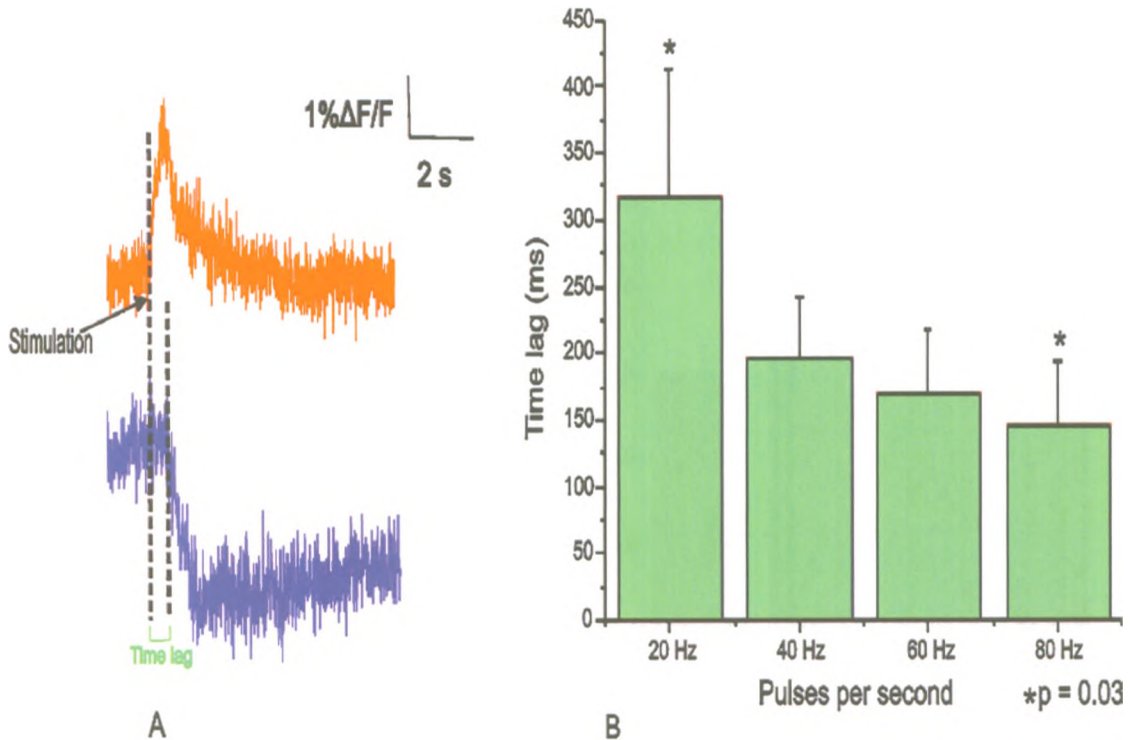
Figure 9- The timing of the excitatory response precedes the inhibitory response in control slices.

(A) The red and blue signals represent the excitatory and inhibitory responses in layers II and III respectively. Lateral olfactory tract stimulation first evokes the excitatory response in layer II and then the activity propagates to the layer III. (B) The inhibitory response latency decreases with higher stimulus frequencies. We compared the average lag time (ms) between the excitatory and inhibitory responses in recordings made after different stimulus frequencies (n= 12 slices from 7 rats). The statistical analysis was done using one-way ANOVA followed by Post hoc analysis.
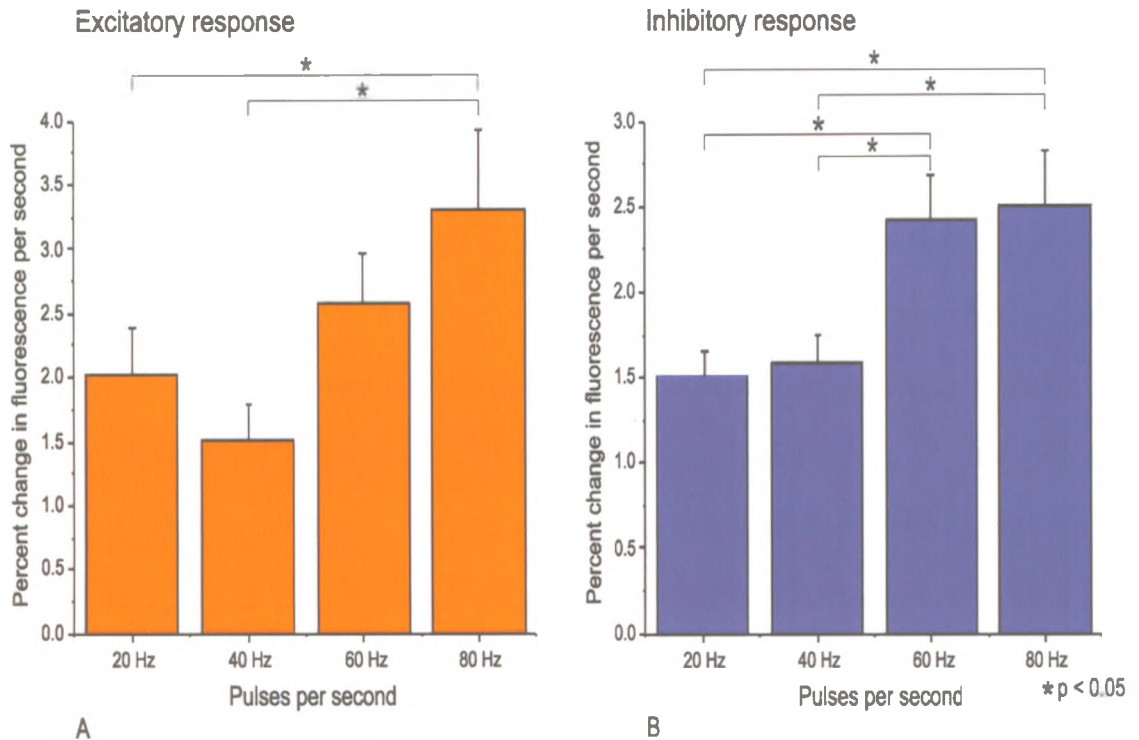
Figure 10- The response rate of both excitatory and inhibitory responses increases with higher frequencies of stimulus in control slices.

The peak fluorescence amplitude from a region of interest was divided by the 10-90% rising time of the same region to measure the response rate after stimulation. (A) The response rate of excitatory activity increases with higher frequencies of stimulus (n= 13 slices from 7 rats). (B) The response rate of inhibitory activity increases with higher stimulus frequencies (n= 10 slices from 7 rats). The statistical analysis was done using one-way ANOVA followed by Post hoc analysis.

To determine the effect of inhibition on the propagation of the activity in PC, we conducted some experiments before and after incubating the slice with 500 nM of gabazine for 15 min. SR95531 (gabazine) is a $GABA_A$-receptor antagonist. We compared the excitatory and inhibitory responses in recordings made before and after applying gabazine. Gabazine made two kinds of effects on the excitatory activity in layer II of control slices. The data showed that gabazine increased the excitatory response in layer II significantly in a group of slices (n= 5 slices from 4 rats, $p = 0.008$, Figure 11A1), whereas it didn't have any effect in another group of slices (n= 8 slices from 5 rats, $p = 0.5$, Figure 11A2). Gabazine also decreased the inhibitory response in layer III of piriform cortex in control rats slices (n= 10 slices from 6 rats, $p = 0.002$, Figure 11B).

In the next step, in order to better understand the circuitry of cells in PC, we recorded the neuronal activity of the PC before and after cutting the slice below layer II. The results showed that both the excitatory and inhibitory responses decreased significantly after disruption made between layer II and III. (n= 6 slices from 6 rats, $p < 0.05$, Figure 12).
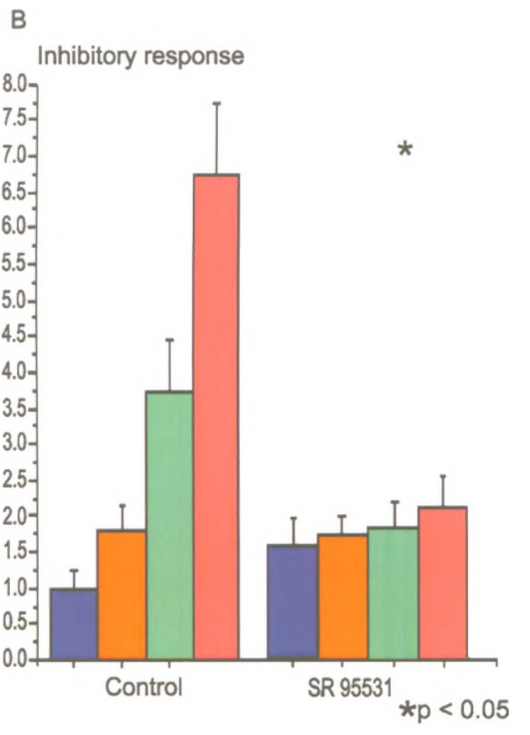
A

Excitatory response

*

*p < 0.05

1

Excitatory response

2

20Hz
40Hz
60Hz
80Hz

B

Inhibitory response

*

*p < 0.05

51
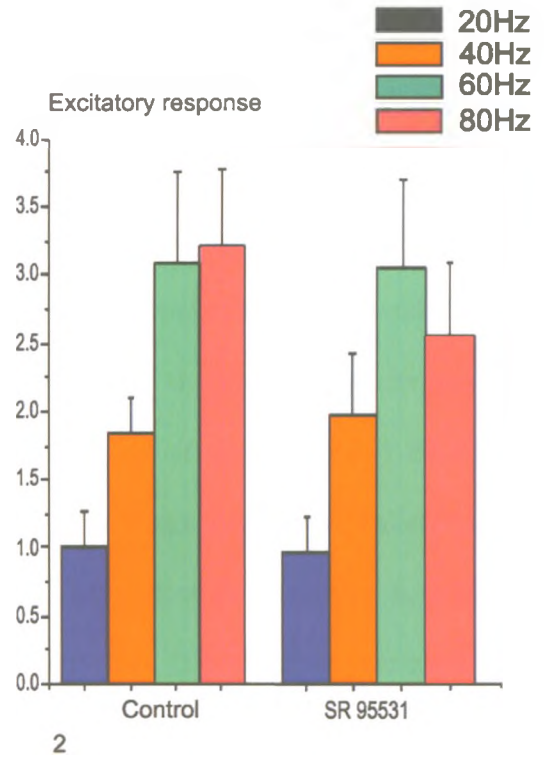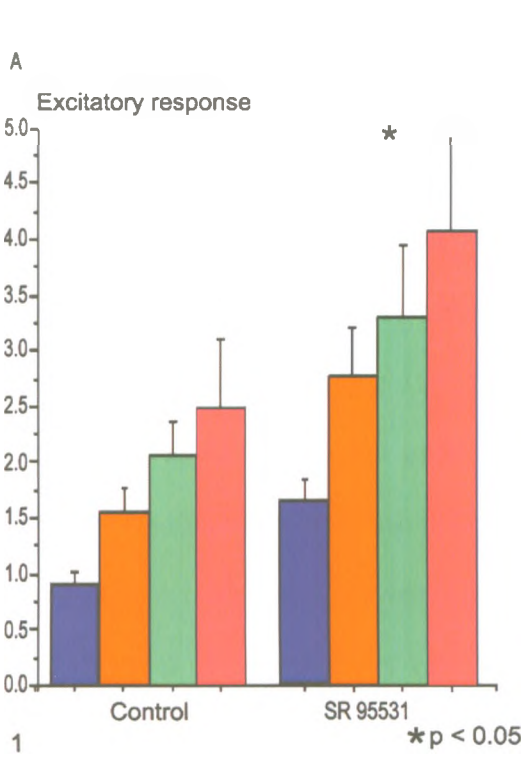
Figure 11- SR95531 alters the excitatory and inhibitory neuronal responses in piriform cortex in control rats.

Brain slices were incubated with 500 nM SR95531 (gabazine) for 15 min. VSDI recordings were made using different stimulus frequencies both before and after applying gabazine. The average peak fluorescence along a 10-pixel stripe in layers II and III was calculated for each recording (see methods). Statistical analysis was performed by normalizing all data with the peak amplitude of 20 Hz stimulation. (A1) SR95531 enhances the excitatory response in layer II of piriform cortex in a group of slices (n= 5 slices from 4 rats). (A2) Gabazine does not have any effect on excitatory activity in another group of control slices (n= 8 slices from 5 rats). (B) SR95531 decreases the inhibitory response in layer III (n= 10 slices from 6 rats). The statistical analysis was done using repeated measures ANOVA.

A

Before cut

0 s

2.13 s

Stripe   Layer III   Layer II

Layer II

Layer III

B

After cut

0 s

2.13 s

Stripe

cut

Stripe

1%ΔF/F

5 s

C

1   **Excitatory response**

percent change in peak amplitude

*

2.5

2.0

1.5

1.0

0.5

0.0

Before cut   Cut   *p < 0.05

2   **Inhibitory response**

percent change in peak amplitude

*

1.5

1.0

0.5

0.0

Before cut   Cut   *p < 0.05
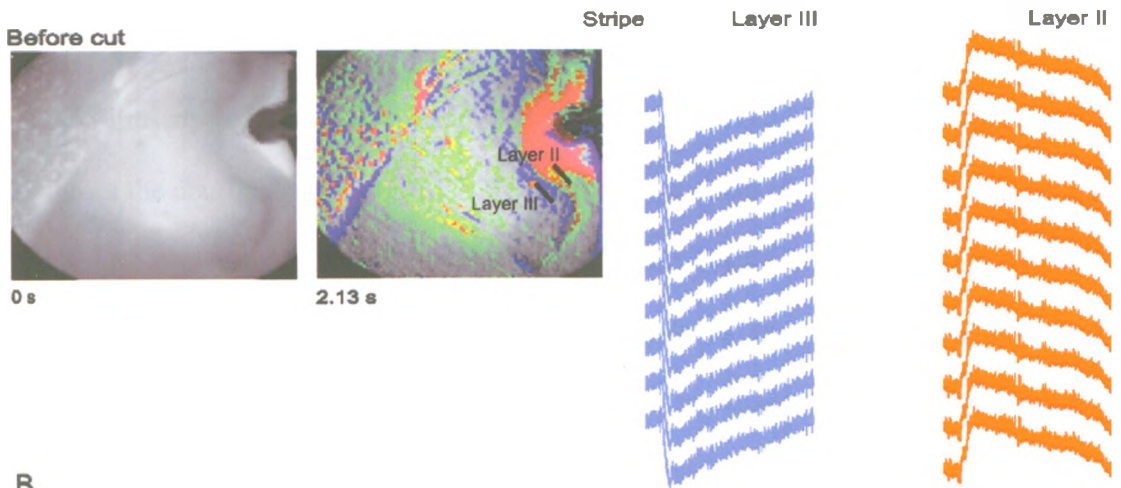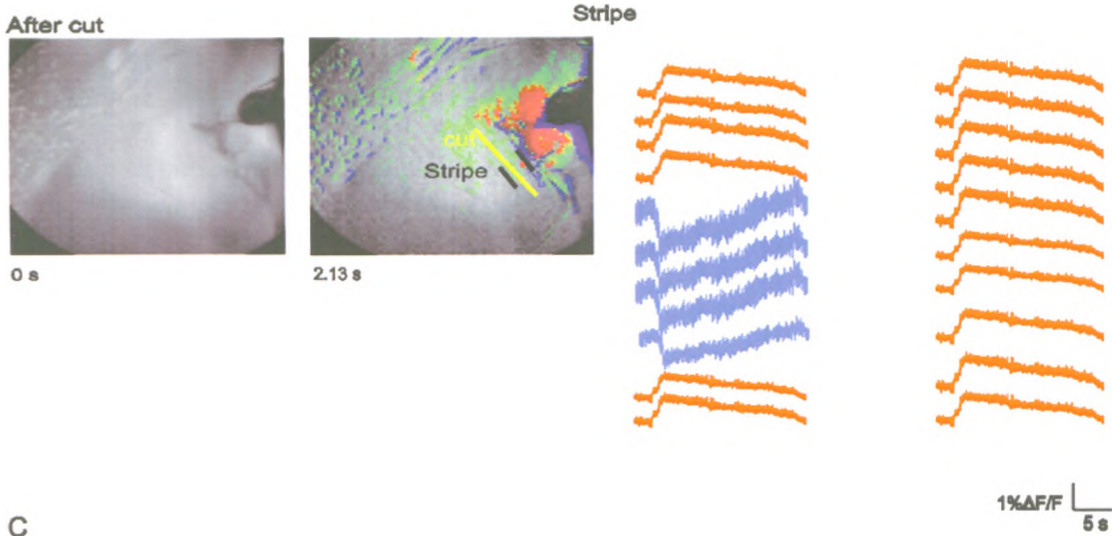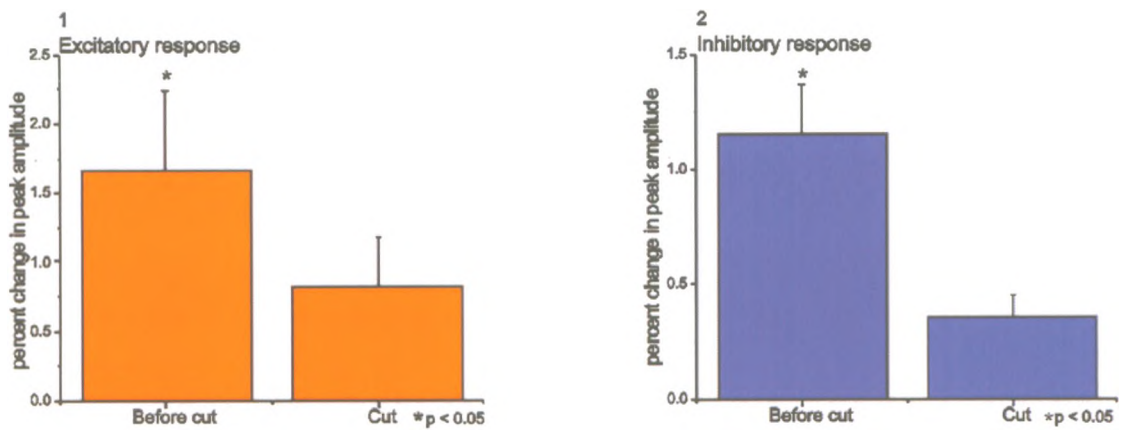
Figure 12- The cut made at the border of layer II and III of piriform cortex decreases the excitatory and inhibitory responses in layers II and III.

(A) Filmstrips of VSDI before and 2.13 s after stimulation. The stripe placed on layer III shows the neuronal activity, which predominantly consists of inhibitory responses. (B) Filmstrips of the same slice after cutting the slice below layer II before and after stimulation. The stripe is placed on the same region as shown in A. The inhibitory responses decrease after cut as some of the pixels show excitatory response and the amplitude of inhibitory responses is smaller. (C1) The peak fluorescence amplitude of excitatory responses decreases after the cut. (C2) The peak fluorescence amplitude of inhibitory responses decrease after the cut (n= 6 slices from 6 rats). The statistical analysis was performed using paired t-test.

Since amygdala kindling has been shown to make long-term changes in the brain circuitry (Goddard et al., 1969;McIntyre & Goddard, 1973;Racine, 1972a), to determine the effect of kindling on the neuronal circuitry in piriform cortex, we repeated some of the experiments in the kindled rats' slices. Electrical stimulus to the LOT in kindled slices induced two kinds of responses in piriform cortex: inhibitory and excitatory responses. Similarly to control slices, the excitatory responses were mostly seen in layer II of PC and EN, whereas the inhibitory responses were mainly located in layer III of PC. Then we investigated the relationship between different stimulus frequencies and the evoked responses in layers II and III of piriform cortex in kindled rats. The data demonstrated linear increase in both excitatory and inhibitory responses in the range of 10-80 pulses per second in kindled rats (excitatory response: n= 6 slices from 5 kindled rats, $p = 0.005$, R= 0.993, Figure 13; inhibitory response: n= 5 slices from 4 kindled rats, $p = 0.005$, R= -0.993, Figure 14).
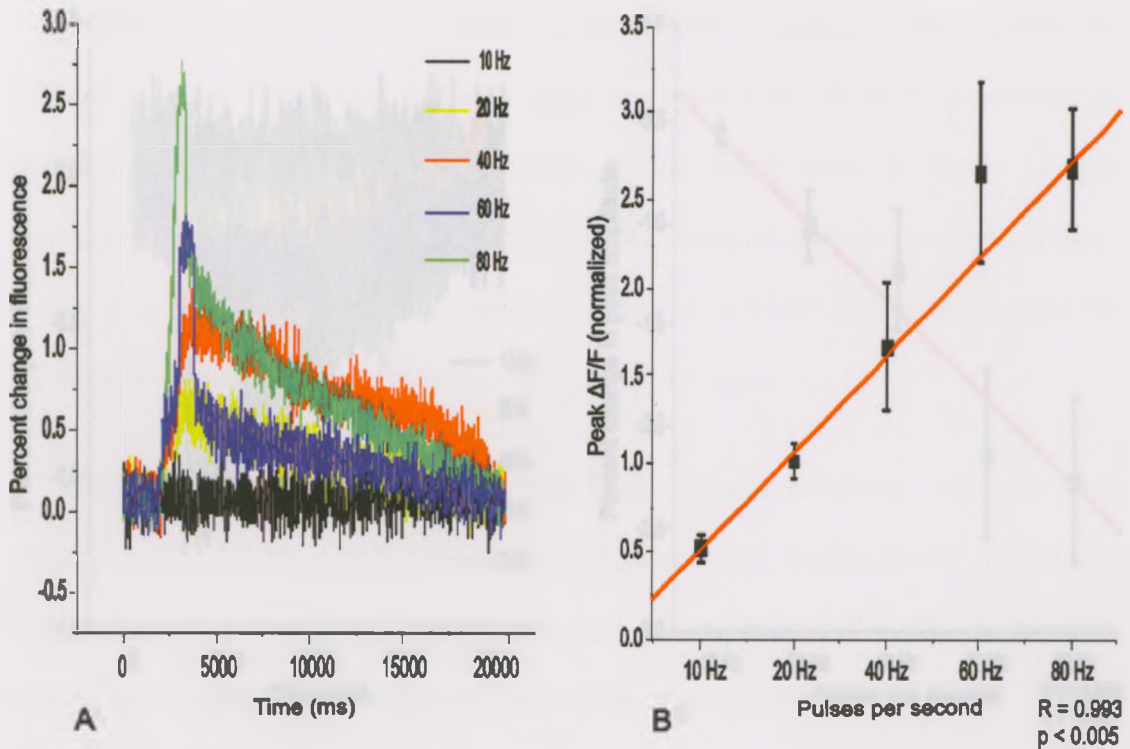
Figure 13- Excitatory response increases linearly over the range of 10-80 Hz in kindled rats.

(A) One second-long trains at different frequencies makes a progressive increase in the excitatory responses. Each wave represents the average change in fluorescence in a ROI placed in layer II of piriform cortex (n= 6 slices from 5 rats). (B) The peak fluorescence response increases in the range of 10-80 pulses per second in a linear manner in kindled rats. The average peak fluorescence for each frequency was normalized by the average peak of 20 Hz. Linear regression analysis was used to fit the line.

Figure 14- Inhibitory response increases linearly over the range of 10-80 Hz in kindled rats.

(A) One second-long trains at different frequencies show a progressive increase in the inhibitory responses. Each wave represents the average change in fluorescence in a ROI placed in layer III of piriform cortex (n= 5 slices from 4 rats). (B) The peak fluorescence response increases in the range of 10 to 80 Hz in a linear manner in kindled rats. The average peak of fluorescence response for each frequency was normalized by the average peak of 20 Hz stimulus. Linear regression analysis was used to fit the line.

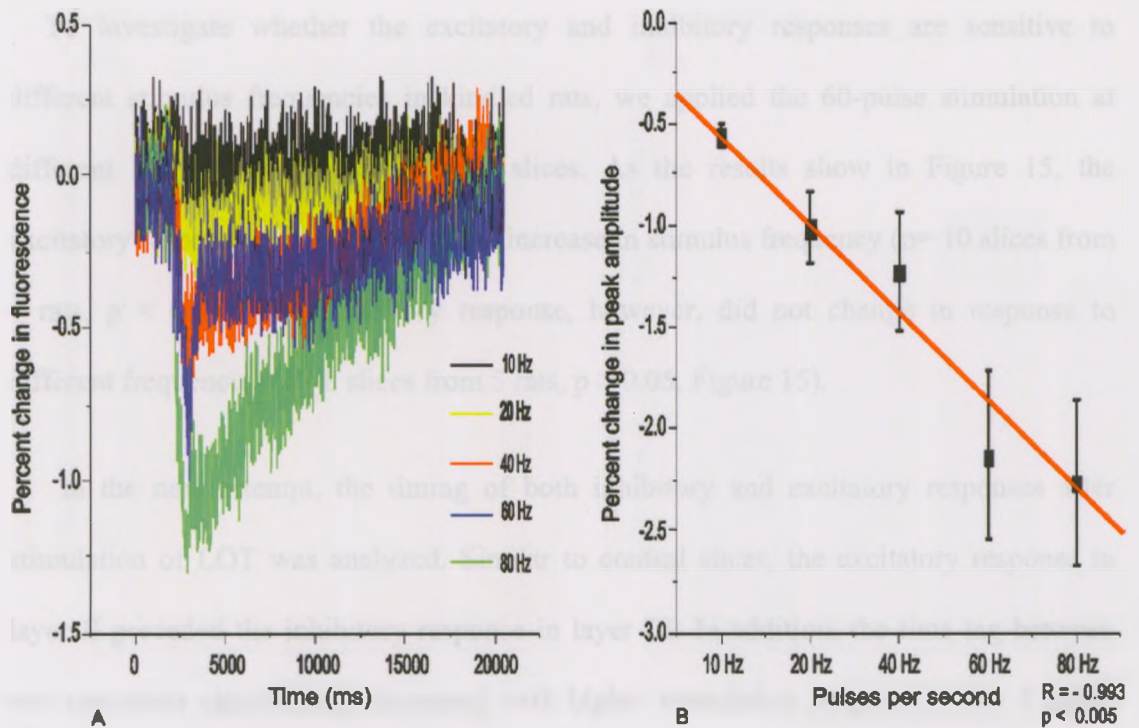To investigate whether the excitatory and inhibitory responses are sensitive to different stimulus frequencies in kindled rats, we applied the 60-pulse stimulation at different frequencies in kindled rats' slices. As the results show in Figure 15, the excitatory response was sensitive to the increase in stimulus frequency (n= 10 slices from 4 rats, p < 0.05). The inhibitory response, however, did not change in response to different frequencies (n= 8 slices from 5 rats, p > 0.05, Figure 15).

In the next attempt, the timing of both inhibitory and excitatory responses after stimulation of LOT was analyzed. Similar to control slices, the excitatory response in layer II preceded the inhibitory response in layer III. In addition, the time lag between two responses significantly decreased with higher stimulation frequencies (n= 9 slices from 4 rats, p < 0.05, Figure 16).

To determine the response rate of two responses, we measured the rate of fluorescence change ($\Delta F/F\%$ / ms) in recordings made with different stimulus frequencies. The results demonstrated that the response rate of neither excitatory nor inhibitory responses were sensitive to stimulus rate in kindled rats (excitatory response: n= 9 slices from 4 rats; inhibitory responses: n= 9 slices from 4 rats, Figure 17). This is in contrast with the results from control slices, in which the higher stimulus frequencies increased the response rate significantly.
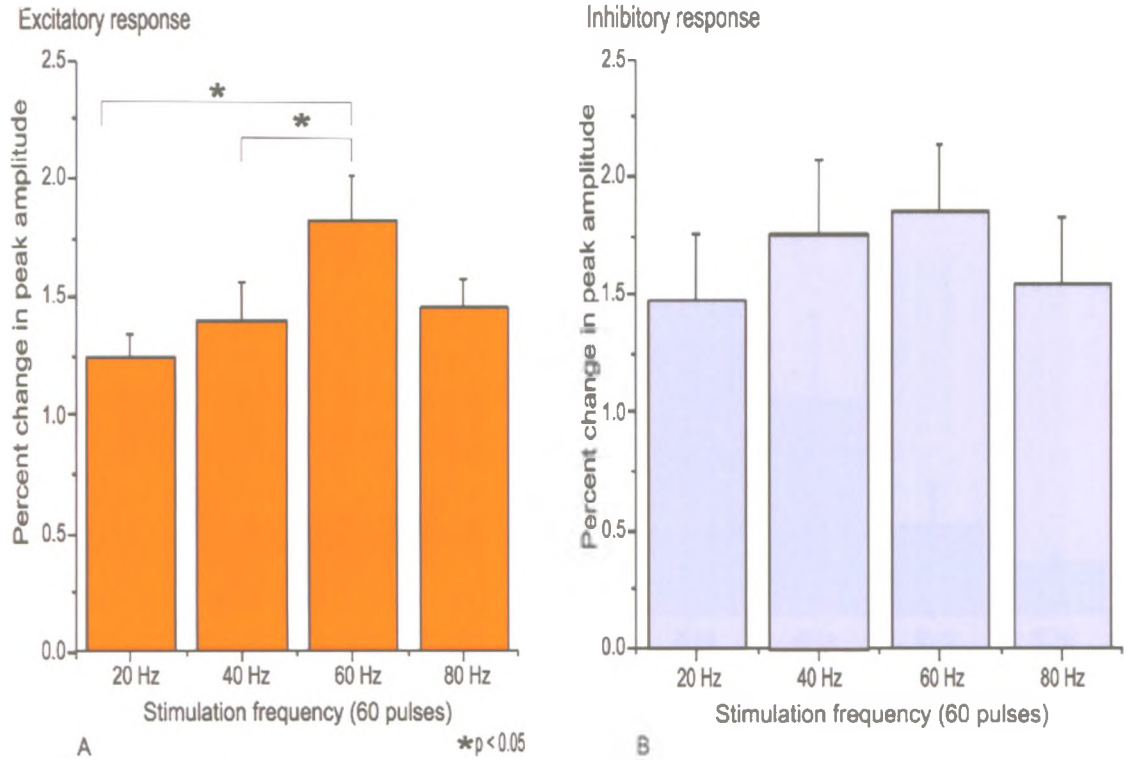
Figure 15- Differential sensitivity to stimulus frequency between excitatory and inhibitory responses in kindled slices.

To test if responses are sensitive to different stimulus frequencies, 60 pulses were applied to the slices at different frequencies. A 10 pixel-stripe was used to calculate the average change in peak fluorescence in each recording. All data were normalized by the peak of 20 Hz stripes (A) Excitatory responses were sensitive to increased stimulus frequency from 20 Hz to 60 Hz (n= 10 slices from 4 rats). (B) Inhibitory responses were not sensitive to stimulus frequency (n= 8 slices from 5 rats). The statistical analysis was done using one-way ANOVA followed by Post hoc analysis.
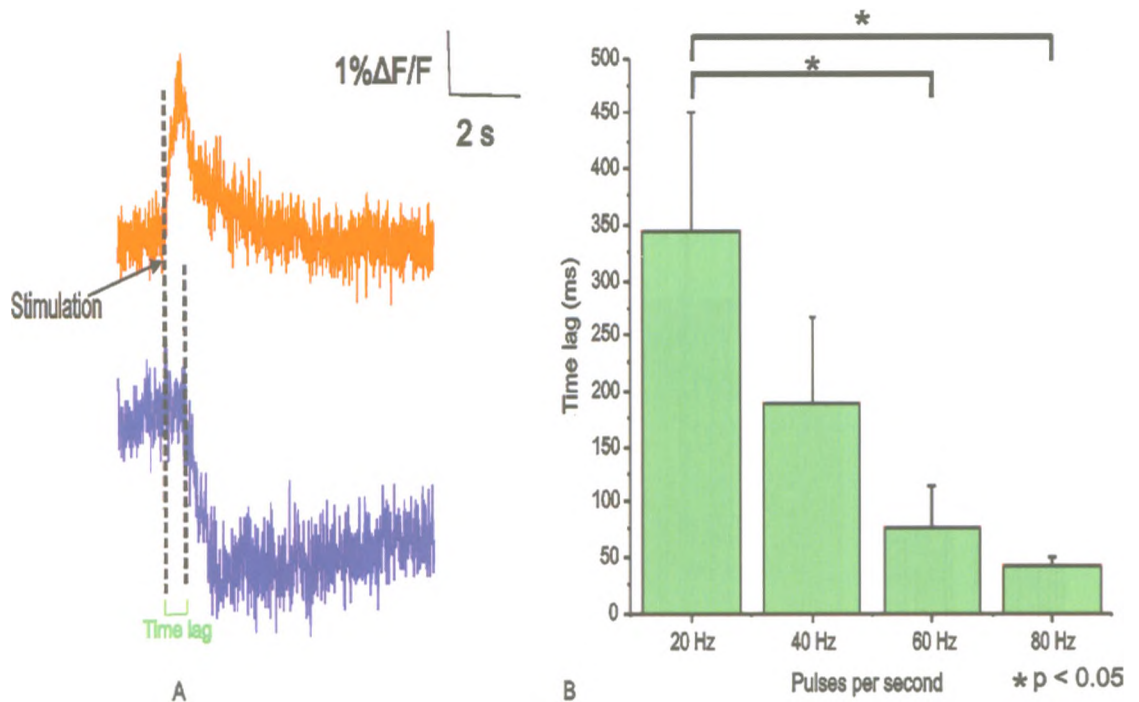
Figure 16- The timing of the excitatory response precedes the inhibitory response in kindled slices.

(A) The red and blue signals represent the excitatory and inhibitory responses in layers II and III, respectively. Lateral olfactory tract stimulation first evokes the excitatory response in layer II and then propagates to the layer III. (B) The inhibitory response latency decreased with higher frequencies of stimulus. We compared the average lag time (ms) between the excitatory and inhibitory response in recordings made with different stimulus frequencies (n= 9 slices from 4 rats). The statistical analysis was done using one-way ANOVA followed by Post hoc analysis.

Excitatory response

Inhibitory response

A

B
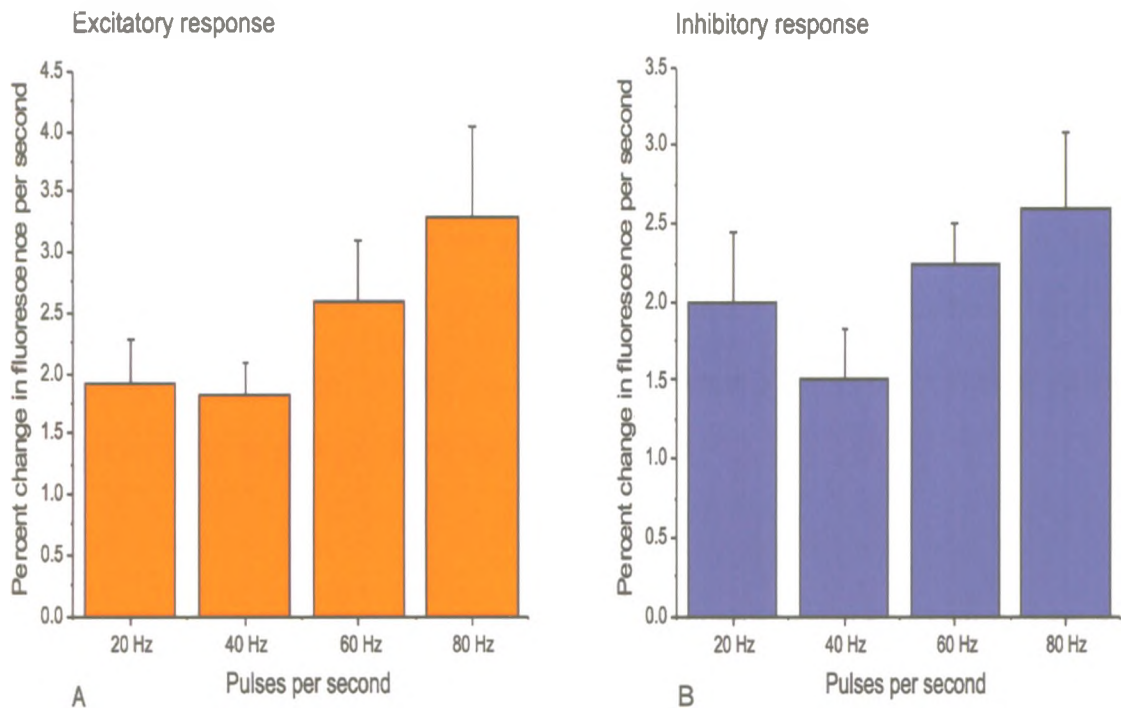
Figure 17- The response rate of both excitatory and inhibitory responses does not change with higher frequency stimuli in kindled rats' slices.

The peak fluorescence amplitude of a region of interest was divided by the 10-90% rising time from the same region to measure the response rate of fluorescence. (A) The response rate of excitatory activity is not sensitive to different stimulus frequencies (n= 9 slices from 4 rats). (B) The response rate of inhibitory activity in kindled rats does not change in response to higher stimulation frequencies (n= 9 slices from 4 rats). The statistical analysis was done using one-way ANOVA followed by Post hoc analysis.

Finally, we measured the effect of gabazine (SR95531) on the neuronal activity in kindled rats. The recordings were made before and after incubating the slices with gabazine (500 nM) (see Figure 18). In contrast with control slices, the excitatory response in kindled slices did not change after gabazine (n= 7 slices from 5 rats, $p = 0.6$). The inhibitory response also didn't change after applying gabazine (n= 8 slices from 5 rats, $p = 0.6$). Thus, we concluded that the excitatory and inhibitory responses in kindled slices were not sensitive to gabazine anymore.
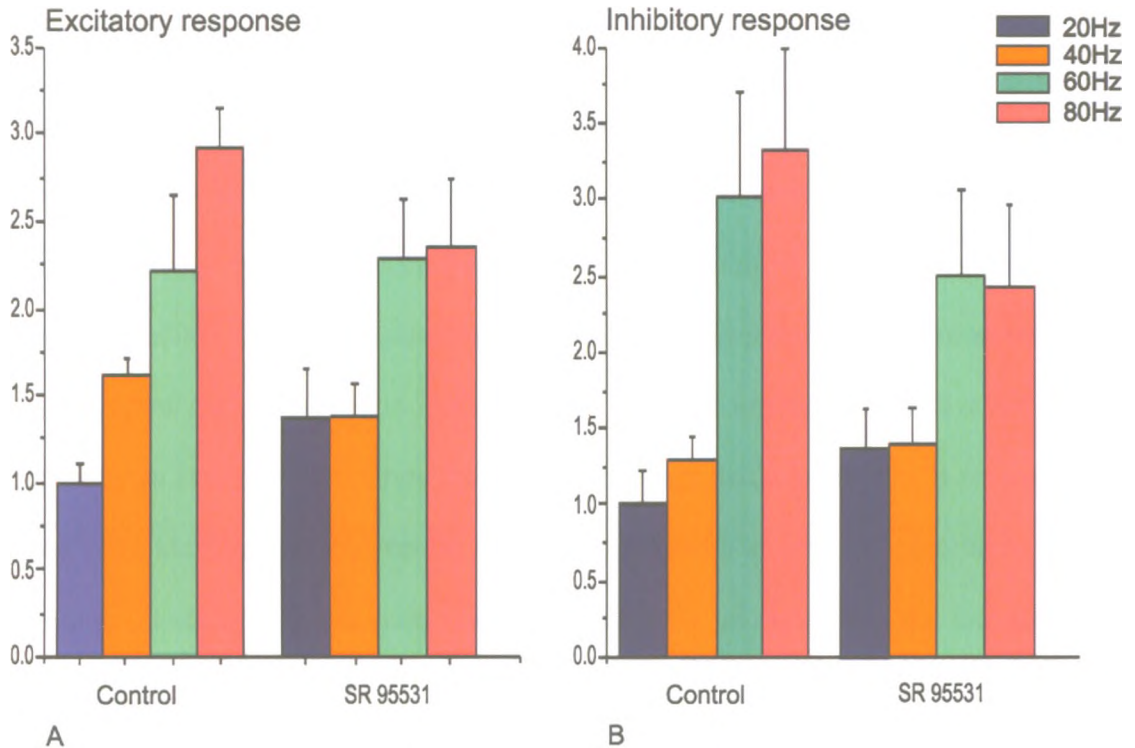
Figure 18- SR95531 does not alter the excitatory and inhibitory responses in piriform cortex in kindled rats.

Brain slices were incubated with 500 nM SR95531 (gabazine) for 15 min. VSDI recordings were made using different frequencies of stimuli both before and after applying gabazine. The average peak fluorescence along a 10-pixel stripe in layers II and III was calculated for each recording (see methods). Statistical analysis was performed by normalizing all data with the peak amplitude of 20 Hz stimulation. (A) SR95531 does not affect the excitatory response in layer II of piriform cortex in kindled rats (n= 7 slices from 5 rats). (B) The inhibitory response in layer III doesn't change in kindled rats after applying gabazine (n= 8 slices from 5 rats). The statistical analysis was done using repeated measures ANOVA.

5. Discussion

In this set of experiments we showed that voltage-sensitive dye imaging could provide a novel insight on neuronal population activity in piriform cortex. High spatial and temporal resolution of VSD recordings enables us to follow the change in the fluorescence emitted from dye molecules residing in cells membranes. We also showed that the occurrence of disinhibition in the layer III of PC is important for activation of principle cells in layer II. Considering the previous findings that inhibitory cells are more inhibited after kindling and the results of this study which imply the importance of disinhibition in driving the activity in principle cells, we propose that increased disinhibition is one of the mechanisms responsible for seizure activity after kindling. This finding is novel, since it is the first time that increased level of inhibition in PC has been implicated in kindling process.

In our recordings, applying the electrical stimulation to LOT lead to propagation of activity downstream to the layers I, II and III of PC. This was similar to the results of previous VSD recordings where the stimulus applied to LOT or Layer I of guinea pig and rat slices *in vitro* spread over the same area (Demir et al., 1998c;Sugitani et al., 1994a). In addition, *in vivo* VSD recordings of rat piriform cortex after stimulation of LOT showed the same propagation pattern from layer I to layer III (Litaudon et al., 1997).

We recorded two main types of fluorescence responses in different layers of PC. The excitatory response, which was reflected by decreased fluorescence intensity signal and the inhibitory response, which was indicated by increased fluorescence signal. The excitatory responses were mostly observed in layers I, and II while the inhibitory

responses were predominantly located in layer III of PC. The activity of the excitatory responses was consistent with previous VSDI studies in PC in which excitation was the only response recorded in the PC after electrical stimulation (Demir et al., 1998c;Litaudon et al., 1997;Sugitani et al., 1994a). The inhibitory response, however, was never described in the PC using VSDI techniques. This was true not only for the PC but also for the other structures such as hippocampus (Plenz & Aertsen, 1993). It was only until recently that a few investigators could record the inhibitory response in hippocampus using optical techniques (Tominaga et al., 2000;Carlson & Coulter, 2008;Coulter & Carlson, 2007). In a study performed in rats' hippocampal slices the inhibitory activity was shown in the stratum radiatum after electrical stimulation of temporoammonic region (Ang et al., 2006;Canepari et al., 2010). The probable reason why previous investigators were unable to record the inhibitory response using VSDI can be explained by the fact that VSDI technique has been improved in recent decades by introduction of new styryl dyes with less toxicity and faster response time.

There is solid evidence suggesting the authenticity of VSD signal as a reliable tool to follow the changes in the membrane potential. Several studies have shown that VSD signals coincide with local field potentials and whole-cell patch clamp recordings. For instance, in a study on PC, it has been shown that after stimulating layer III of PC, the maximum negativity in the field potential in the claustrum coincides well with the peak of excitatory fluorescence response from the same region (Demir et al., 1998c). Another study performed on hippocampus also demonstrated the overlap of an excitatory fluorescence response on a dendritic I-clamp recording from a CA1 pyramidal cell (Carlson & Coulter, 2008). Therefore, based on all these observations we suggest that

65

excitatory and inhibitory responses recorded by VSDI represent the average change in membrane voltage in-group of cells in the recorded area. This average response would be confused with excitatory and inhibitory signals of VSD recorded from a single cell that has been injected with the dye, which can reveal both EPSPs and IPSPs (Canepari et al., 2010;Grinvald & Farber, 1981;Grinvald et al., 1983).

In the next set of experiments we found that the excitatory responses were sensitive to an increase in the frequency of stimulation from the LOT over the beta (10-20 Hz) and gamma range (30-80 Hz), a range of action potential frequencies that is typical of the olfactory bulb communication with the PC (Boeijinga & Lopes da Silva, 1988;Bressler, 1984;Freeman, 1959;Freeman, 1978;Kay & Freeman, 1998). For example, gamma oscillations that originate in the PC are thought to originate as the result of feedback between excitatory pyramidal cells and inhibitory INs (Freeman, 1974;Rall & Shepherd, 1968;Litaudon et al., 2008). We also know any disruption in the gamma frequency from the OB will also abolish oscillations in PC (Becker & Freeman, 1968). Thus, any stimulus in the gamma and beta range applied to the LOT can facilitate the excitatory response in the PC. This was not apparently the case with the inhibitory responses in the layer III as they were not sensitive to increasing frequency stimulation, even though their amplitude increased by higher number of pulses per second. Thus, the inhibition was only sensitive to the strength of stimuli but not the frequency of it. This may be due to the fact that interneurons fire high frequency bursts of action potentials that would not necessarily encode the frequency of stimulus. Recent data from our lab has indicated that some interneurons may fire as fast as 150 Hz. Thus, once threshold is reached the neuron will fire more frequently than the stimulus that was provided. As well interneurons have

a predominate NMDA receptor mediated synaptic component which is slowly developing and long lasting and would tend to be insensitive to frequency (Dingledine et al., 1999b).

Analyzing the timing of excitatory and inhibitory responses revealed that the inhibitory responses were activated after the excitatory responses. This can be explained by the fact that any stimulation to the LOT directly activates the apical dendrites of pyramidal cells in layers I and II which if sufficiently intense causes action potentials that will stimulate local circuit interneurons in layer III (Haberly & Bower, 1984;Loscher & Ebert, 1996b). We also noticed that stimulating the LOT with more pulses per second lead to a significant decrease in the time lag, which is consistent with a previous VSD study showing higher stimulus intensity, decreased the latency to response in the PC (Demir et al., 1998). Increasing the intensity of stimulation with higher pulses also resulted in a faster change in fluorescence activity or faster response rate in control slices.

Our data also showed that cutting the slice just below layer II of PC resulted in significant decrease in both excitatory and inhibitory responses, implying the pivotal role of feed forward and feedback interaction between layers II and III cells to maintain the synchronized activity of the PC. In a basic circuit of the PC stimulation of LOT activates the interneurons in layer I which provides feed forward inhibition to pyramidal cells (Kanter & Haberly, 1990), also pyramidal cells can activate interneurons in layer III which provide feedback inhibition on the pyramidal cells (Haberly & Behan, 1983). Based on our observations it is likely that activation of layer III interneurons may feed back to inhibit other interneurons that control pyramidal cells excitability. Therefore, the

occurrence of disinhibition in layer III leads to excitation of pyramidal cells in layer II (see Figure 19).

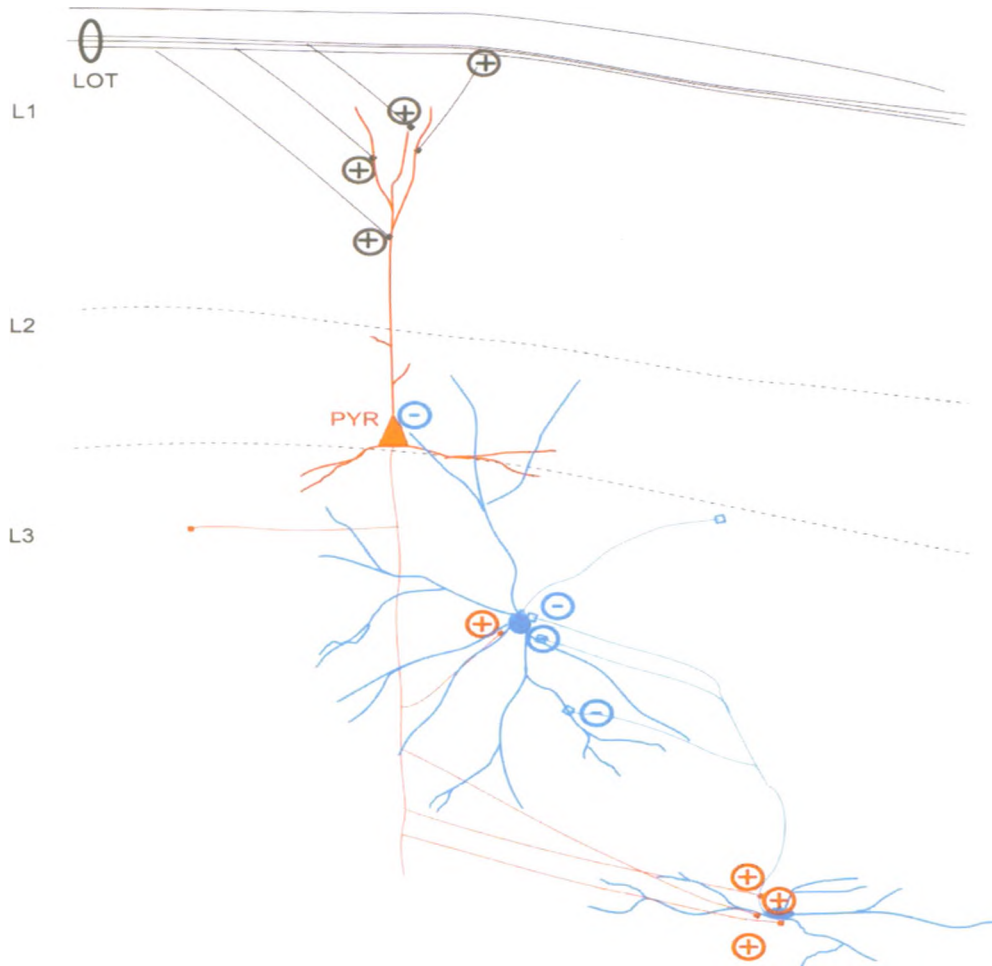**Figure 19- Schematic diagram showing the postulated circuitry in the PC.**

Excitatory and inhibitory synapses are shown with positive and negative symbols. The afferent input from LOT activates the pyramidal cell in the layer II. Pyramidal cell makes excitatory connections on an interneuron in layer III. The activated interneuron feedbacks to inhibit the interneuron that controls the pyramidal cell excitability.

We were also interested to find out how kindling alters the circuitry of the PC. To investigate the effects of kindling on PC, some of the experiments were performed in the kindled rats' slices as well. The two main responses, excitatory and inhibitory, were also present in the kindled rats. Similar to control slices, increasing the stimulus intensity by higher pulses per second enhanced both kinds of responses in kindled rats. Kindled slices also showed the same pattern of sensitivity to differing stimulus frequency, where the excitatory responses were sensitive to higher frequencies in contrast to inhibitory responses. Nevertheless, there were some differences between control and kindled recordings. First, the time lag between the excitatory and inhibitory responses was smaller in kindled rats, especially with higher frequency stimuli. The average time lag between the two responses after 80 Hz stimuli was significantly shorter in kindled rats. The reason for this is not readily clear but it may be due to altered synaptic strength by the excitatory input from the LOT. Alternatively, we have shown that inhibition among interneurons is increased after kindling, suggesting of increased disinhibition in layer II of PC that may explain our observations (Gavrilovici et al., 2006). Second, in contrast to control slices the response rate of excitatory and inhibitory activities in kindled rats did not increase with higher pulses of stimulus. This agrees with the findings of a previous study in the PC which showed that after kindling the interneurons were more inhibited, consequently leading to disinhibition of pyramidal cells in the layer II (Gavrilovici et al., 2006). Based on those findings we can assume that since the pyramidal cells in the layer II of PC were disinhibited after kindling, they were already firing with maximum rate; hence, increasing the input frequency did not make any change in the response time. The interneurons are also more inhibited after kindling.

Third, decreasing the inhibition by applying 500 nM gabazine (SR95531), a $GABA_A$-receptor antagonist, made different effects in control and kindled rats. Gabazine increased the excitatory responses in a group of slices and decreased the inhibitory responses in control rats. Other VSD studies performed either in hippocampus or in the PC also showed that applying bicuculline, another $GABA_A$-receptor antagonist (1 or 5 µm), to the control slices enhanced the excitatory response (Demir et al., 2000;von et al., 2011). However, gabazine did not affect the excitatory response in another group of slices. This can be explained by considering the effect of disinhibition on the firing of pyramidal cells. We propose that any stimulus to the LOT can activate the interneurons in layer III. Then, interneurons can make inhibitory feedback synapses on other interneurons which control the pyramidal cells firing; therefore, blocking the $GABA_A$ receptor on pyramidal cells increased the excitatory response in layer II, while blocking the same receptors on INs which control pyramidal cells activity resulted in decreased inhibitory input to the pyramidal cells. Thus, these contraindicating effects of gabazine can explain its different effects on excitatory activity in layer II.

In kindled rats the inhibitory and excitatory responses did not change in response to gabazine. This is consistent with our previous finding implying the enhancement of disinhibition in piriform cortex after kindling. Thus, decreasing the inhibition cannot affect the excitatory response because the pyramidal cells were already disinhibited after kindling.

In conclusion, our results suggest that VSD imaging can be used to follow the changes in the membrane potential in multiple sites of PC simultaneously. The only concern

about the VSDs is the effect of dye on membrane channels. It has been shown that acute use of dye potentiates $GABA_A$ receptors; however, this effect was completely reversible after washing out the dye (Mennerik et al., 2010). Since in our experiments the slices were washed with choline solution for 15 min before recording and also during the recording; we believe the dye had no effect on the membrane channels. VSDI also provides the opportunity to analyze the behaviour of different cells in the PC circuitry in different conditions such as kindling. In addition, we demonstrated the important role of interneurons in regulating the firing of principle cells in the PC. Based on present observations, we can argue that inhibitory synapses on interneurons that result in disinhibition in layer III are important for activation of principle cells. Furthermore, our results imply that the level of disinhibition is increased after kindling. Although this may not be the only mechanism of seizure propagation in epilepsy, it gives us a new insight into the mechanism of seizure. In contrast to traditional belief that decreased level of inhibition is responsible for seizure activity, here we have shown that enhancement of inhibition among the interneurons can facilitate the seizure activity. This is important since many drugs target to increase the inhibitory activity have not been successful or just made partial effects in patients with temporal lobe epilepsy. More investigation in this field can lead to introduction more effective drugs for the epileptic patients.

6. Reference List

1.   Ang CW, Carlson GC, & Coulter DA (2005). Hippocampal CA1 circuitry dynamically gates direct cortical inputs preferentially at theta frequencies. *J Neurosci* **25**, 9567-9580.

2.   Ang CW, Carlson GC, & Coulter DA (2006). Massive and specific dysregulation of direct cortical input to the hippocampus in temporal lobe epilepsy. J Neurosci 26, 11850-11856.

3.   Ascoli GA, Alonso-Nanclares L, Anderson SA, Barrionuevo G, Benavides-Piccione R, Burkhalter A, Buzsaki G, Cauli B, DeFelipe J, Fairen A, Feldmeyer D, Fishell G, Fregnac Y, Freund TF, Gardner D, Gardner EP, Goldberg JH, Helmstaedter M, Hestrin S, Karube F, Kisvarday ZF, Lambolez B, Lewis DA, Marin O, Markram H, Munoz A, Packer A, Petersen CC, Rockland KS, Rossier J, Rudy B, Somogyi P, Staiger JF, Tamas G, Thomson AM, Toledo-Rodriguez M, Wang Y, West DC, & Yuste R (2008). Petilla terminology: nomenclature of features of GABAergic interneurons of the cerebral cortex. Nat Rev Neurosci 9, 557-568.

4.   Bakker R, Schubert D, Levels K, Bezgin G, Bojak I, & Kotter R (2009). Classification of cortical microcircuits based on micro-electrode-array data from slices of rat barrel cortex. Neural Netw 22, 1159-1168.

5.   Ballain T, Litaudon P, Martiel JL, & Cattarelli M (1998). Role of the net architecture in piriform cortex activity: analysis by a mathematical model. Biol Cybern 79, 323-336.

6.   Bayraktar T, Welker E, Freund TF, Zilles K, & Staiger JF (2000). Neurons immunoreactive for vasoactive intestinal polypeptide in the rat primary somatosensory cortex: morphology and spatial relationship to barrel-related columns. J Comp Neurol 420, 291-304.

7.   Beaulieu C & Somogyi P (1991). Enrichment of cholinergic synaptic terminals on GABAergic neurons and coexistence of immunoreactive GABA and choline acetyltransferase in the same synaptic terminals in the striate cortex of the cat. J Comp Neurol 304, 666-680.

8.   Becker CJ & Freeman WJ (1968). Prepyriform electrical activity after loss of peripheral or central input, or both. Physiol Behav 597-599.

9.   Ben-Ari Y (1985). Limbic seizure and brain damage produced by kainic acid: mechanisms and relevance to human temporal lobe epilepsy. Neurosci 14, 375-403.

10.   Ben-Ari Y, Lagowska J, Tremblay E, & Le Gal La SG (1979). A new model of focal status epilepticus: intra-amygdaloid application of kainic acid elicits repetitive secondarily generalized convulsive seizures. Brain Res 163, 176-179.

11.   Benson DL, Isackson PJ, & Jones EG (1991). In situ hybridization reveals VIP precursor mRNA-containing neurons in monkey and rat neocortex. Brain Res Mol Brain Res 9, 169-174.

12.   Bertram E (2007). The relevance of kindling for human epilepsy. Epilepsia 48 Suppl 2, 65-74.

13.   Biella G, Spaiardi P, Toselli M, de CM, & Gnatkovsky V (2010). Functional interactions within the parahippocampal region revealed by voltage-sensitive dye imaging in the isolated guinea pig brain. J Neurophysiol 103, 725-732.

14.   Boeijinga PH & Lopes da Silva FH (1988). Differential distribution of beta and theta EEG activity in the entorhinal cortex of the cat. Brain Res 448, 272-286.

15.   Bonhoeffer T & Staiger V (1988). Optical recording with single cell resolution from monolayered slice cultures of rat hippocampus. Neurosci Lett 92, 259-264.

16.   Bonhoeffer T, Staiger V, & Aertsen A (1989). Synaptic plasticity in rat hippocampal slice cultures: local "Hebbian" conjunction of pre- and postsynaptic stimulation leads to distributed synaptic enhancement. Proc Natl Acad Sci U S A 86, 8113-8117.

17.   Bressler SL (1984). Spatial organization of EEGs from olfactory bulb and cortex. Electroencephalogr Clin Neurophysiol 57, 270-276.

18.   Buzsaki G & Chrobak JJ (1995). Temporal structure in spatially organized neuronal ensembles: a role for interneuronal networks. Curr Opin Neurobiol 5, 504-510.

19.   Buzsaki G & Traub RD (2008). Physiologic basis of the electroencephalic and local field potentials. In Epilepsy: a comprehensive textbook, eds. Engel J & Pedley T.A., pp. 797-807. Lippincott Williams& Willkins.

20.   Buzsaki G (2002). Theta oscillations in the hippocampus. Neuron 33, 325-340.

21.   Buzsaki G, Geisler C, Henze DA, & Wang XJ (2004). Interneuron Diversity series: Circuit complexity and axon wiring economy of cortical interneurons. Trends Neurosci 27, 186-193.

22.   Callaway EM & Yuste R (2002). Stimulating neurons with light. Curr Opin Neurobiol 12, 587-592.

23.   Canepari M, Willadt S, Zecevic D, & Vogt KE (2010). Imaging inhibitory synaptic potentials using voltage sensitive dyes. Biophys J 98, 2032-2040.

24.   Carlson GC & Coulter DA (2008). In vitro functional imaging in brain slices using fast voltage-sensitive dye imaging combined with whole-cell patch recording. Nat Protoc 3, 249-255.

25.   Catterall WA (1981). Localization of sodium channels in cultured neural cells. J Neurosci 1, 777-783.

26.   Cavalheiro EA, Leite JP, Bortolotto ZA, Turski WA, Ikonomidou C, & Turski L (1991). Long-term effects of pilocarpine in rats: structural damage of the brain triggers kindling and spontaneous recurrent seizures. Epilepsia 32, 778-782.

27.   Chapman CA, Xu Y, Haykin S, & Racine RJ (1998). Beta-frequency (15-35 Hz) electroencephalogram activities elicited by toluene and electrical stimulation in the behaving rat. Neuroscience 86, 1307-1319.

28.   Chen LB (1988). Mitochondrial membrane potential in living cells. Annu Rev Cell Biol 4, 155-181.

29.   Chen ZF, Schottler F, Bertram E, Gall CM, Anzivino MJ, & Lee KS (2000). Distribution and initiation of seizure activity in a rat brain with subcortical band heterotopia. Epilepsia 41, 493-501.

30.   Chien CB & Pine J (1991). Voltage-sensitive dye recording of action potentials and synaptic potentials from sympathetic microcultures. Biophys J 60, 697-711.

31.   Chocholova L (1962). The role or the cerebral cortex in audiogenic seizures in the rat. Physiol Bohemoslov 11, 452-457.

32.   Cinelli AR & Kauer JS (1995). Salamander olfactory bulb neuronal activity observed by video rate, voltage-sensitive dye imaging. II. Spatial and temporal properties of responses evoked by electric stimulation. J Neurophysiol 73, 2033-2052.

33.   Cobb SR, Buhl EH, Halasy K, Paulsen O, & Somogyi P (1995). Synchronization of neuronal activity in hippocampus by individual GABAergic interneurons. Nature 378, 75-78.

34.   Cohen LB & Salzberg BM (1978). Optical measurement of membrane potential. Rev Physiol Biochem Pharmacol 83, 35-88.

35.   Cohen LB, Keynes RD, & Hille B (1968). Light scattering and birefringence changes during nerve activity. Nature 218, 438-441.

36.   Cohen LB, Salzberg BM, Davila HV, Ross WN, Landowne D, Waggoner AS, & Wang CH (1974). Changes in axon fluorescence during activity: molecular probes of membrane potential. J Membr Biol 19, 1-36.

37.   Colom LV & Saggau P (1994). Spontaneous interictal-like activity originates in multiple areas of the CA2-CA3 region of hippocampal slices. J Neurophysiol 71, 1574-1585.

38.   Colonnier M & O'Kusky J (1981). [Number of neurons and synapses in the visual cortex of different species]. Rev Can Biol 40, 91-99.

39.   Conti F, DeFelipe J, Farinas I, & Manzoni T (1989). Glutamate-positive neurons and axon terminals in cat sensory cortex: a correlative light and electron microscopic study. J Comp Neurol 290, 141-153.

40.   Conti F, Fabri M, & Manzoni T (1988). Glutamate-positive corticocortical neurons in the somatic sensory areas I and II of cats. J Neurosci 8, 2948-2960.

41.   Cossart R, Bernard C, & Ben Ari Y (2005). Multiple facets of GABAergic neurons and synapses: multiple fates of GABA signalling in epilepsies. Trends Neurosci 28, 108-115.

42.   Cossart R, Dinocourt C, Hirsch JC, Merchan-Perez A, De Felipe J, Ben Ari Y, Esclapez M, & Bernard C (2001a). Dendritic but not somatic GABAergic inhibition is decreased in experimental epilepsy. Nat Neurosci 4, 52-62.

43.   Cossart R, Dinocourt C, Hirsch JC, Merchan-Perez A, De FJ, Ben-Ari Y, Esclapez M, & Bernard C (2001b). Dendritic but not somatic GABAergic inhibition is decreased in experimental epilepsy. Nat Neurosci 4, 52-62.

44.   Coulter DA & Carlson GC (2007). Functional regulation of the dentate gyrus by GABA-mediated inhibition. Prog Brain Res 163, 235-243.

45.   Coulter DA, McIntyre DC, & Loscher W (2002). Animal models of limbic epilepsies: what can they tell us? Brain Pathol 12, 240-256.

46.   Csicsvari J, Hirase H, Czurko A, Mamiya A, & Buzsaki G (1999). Oscillatory coupling of hippocampal pyramidal cells and interneurons in the behaving Rat. J Neurosci 19, 274-287.

47.   Dasheiff RM (1989). Regional voltage map of the hippocampus during seizures. Exp Neurol 105, 189-196.

48.   DeFelipe J & Jones EG (1992). High-Resolution Light and Electron Microscopic Immunocytochemistry of Colocalized GABA and Calbindin D-28k in Somata and Double Bouquet Cell Axons of Monkey Somatosensory Cortex. Eur J Neurosci 4, 46-60.

49.   DeFelipe J, Hendry SH, Jones EG, & Schmechel D (1985). Variability in the terminations of GABAergic chandelier cell axons on initial segments of pyramidal cell axons in the monkey sensory-motor cortex. J Comp Neurol 231, 364-384.

50.   Del Rio MR & DeFelipe J (1994). A study of SMI 32-stained pyramidal cells, parvalbumin-immunoreactive chandelier cells, and presumptive thalamocortical axons in the human temporal neocortex. J Comp Neurol 342, 389-408.

51.   Del Rio MR & DeFelipe J (1997). Colocalization of parvalbumin and calbindin D-28k in neurons including chandelier cells of the human temporal neocortex. J Chem Neuroanat 12, 165-173.

52.   Demir R, Haberly LB, & Jackson MB (1998a). Voltage imaging of epileptiform activity in slices from rat piriform cortex: onset and propagation. J Neurophysiol 80, 2727-2742.

53.   Demir R, Haberly LB, & Jackson MB (1998b). Voltage imaging of epileptiform activity in slices from rat piriform cortex: onset and propagation. J Neurophysiol 80, 2727-2742.

54.   Demir R, Haberly LB, & Jackson MB (1998c). Voltage imaging of epileptiform activity in slices from rat piriform cortex: onset and propagation. J Neurophysiol 80, 2727-2742.

55.   Demir R, Haberly LB, & Jackson MB (2000). Imaging epileptiform discharges in slices of piriform cortex with voltage-sensitive fluorescent dyes. Ann N Y Acad Sci 911, 404-417.

56. Destexhe A & Sejnowski TJ (2003). Interactions between membrane conductances underlying thalamocortical slow-wave oscillations. Physiol Rev 83, 1401-1453.

57. Dingledine R, Borges K, Bowie D, & Traynelis SF (1999a). The glutamate receptor ion channels. Pharmacol Rev 51, 7-61.

58. Dingledine R, Borges K, Bowie D, & Traynelis SF (1999b). The glutamate receptor ion channels. Pharmacol Rev 51, 7-61.

59. Dinocourt C, Petanjek Z, Freund TF, Ben Ari Y, & Esclapez M (2003). Loss of interneurons innervating pyramidal cell dendrites and axon initial segments in the CA1 region of the hippocampus following pilocarpine-induced seizures. J Comp Neurol 459, 407-425.

60. Dori I, Petrou M, & Parnavelas JG (1989). Excitatory transmitter amino acid-containing neurons in the rat visual cortex: a light and electron microscopic immunocytochemical study. J Comp Neurol 290, 169-184.

61. Ebert U, Rundfeldt C, & Loscher W (1995). Development and pharmacological suppression of secondary afterdischarges in the hippocampus of amygdala-kindled rats. Eur J Neurosci 7, 732-741.

62. Eeckman FH & Freeman WJ (1990). Correlations between unit firing and EEG in the rat olfactory system. Brain Res 528, 238-244.

63. Ekstrand JJ, Domroese ME, Feig SL, Illig KR, & Haberly LB (2001). Immunocytochemical analysis of basket cells in rat piriform cortex. J Comp Neurol 434, 308-328.

64. Elias SA, Yae H, & Ebner TJ (1993). Optical imaging of parallel fiber activation in the rat cerebellar cortex: spatial effects of excitatory amino acids. Neurosci 52, 771-786.

65. Emson PC & Lindvall O (1979). Distribution of putative neurotransmitters in the neocortex. Neurosci 4, 1-30.

66. Engel J, Jr. & Pedley T.A. (2008). What Is Epilepsy? In Epilepsy; A Comprehensive Textbook, eds. Engel J, Jr. & Pedley T.A., pp. 1-9. Lippincott Williams& Wilkins, Philadelphia.

67. Engel J, Jr., Wolfson L, & Brown L (1978). Anatomical correlates of electrical and behavioral events related to amygdaloid kindling. Ann Neurol 3, 538-544.

68.   Faingold CL, Anderson CAB, & Caspary DM (1991). Involvement of GABA in acoustically-evoked inhibition in inferior colliculus neurons. Hearing Res 52, 201-216.

69.   Fairen A, DeFelipe J, & Regidor J (1984). Non-pyramidal neurons. In Cerebral cortex, eds. Peters A & Jones EG, pp. 201-253. Plenum Press, New York.

70.   Feldman ML (1984). Morphology of the neocortical pyramidal neuron. In Cerebral Cortex, eds. Peters A & Jones EG, pp. 123-200. Plenum Press, New York.

71.   Fisher RS, van Emde BW, Blume W, Elger C, Genton P, Lee P, & Engel J, Jr. (2005). Epileptic seizures and epilepsy: definitions proposed by the International League Against Epilepsy (ILAE) and the International Bureau for Epilepsy (IBE). Epilepsia 46, 470-472.

72.   Fluhler E, Burnham VG, & Loew LM (1985). Spectra, membrane binding, and potentiometric responses of new charge shift probes. Biochem 24, 5749-5755.

73.   Fox SE (1989). Membrane potential and impedance changes in hippocampal pyramidal cells during theta rhythm. Exp Brain Res 77, 283-294.

74.   Freedman JC & Novak TS (1989). Optical measurement of membrane potential in cells, organelles, and vesicles. Methods Enzymol 172, 102-122.

75.   Freeman WJ (1959). Distribution in time and space of prepyriform electrical activity. J Neurophysiol 22, 644-665.

76.   Freeman WJ (1974). Stability characteristics of positive feedback in a neural population. IEEE Trans Biomed Eng 21, 358-364.

77.   Freeman WJ (1978). Spatial properties of an EEG event in the olfactory bulb and cortex. Electroencephalogr Clin Neurophysiol 44, 586-605.

78.   Freund TF, Martin KA, Smith AD, & Somogyi P (1983). Glutamate decarboxylase-immunoreactive terminals of Golgi-impregnated axoaxonic cells and of presumed basket cells in synaptic contact with pyramidal neurons of the cat's visual cortex. J Comp Neurol 221, 263-278.

79.   Fritschy JM, Kiener T, Bouilleret V, & Loup F (1999). GABAergic neurons and GABA(A)-receptors in temporal lobe epilepsy. Neurochem Int 34, 435-445.

80.   Fromherz P & Vetter T (1992). Cable properties of arborized Retzius cells of the leech in culture as probed by a voltage-sensitive dye. Proc Natl Acad Sci U S A 89, 2041-2045.

81.   Frostig RD, Xiong Y, Chen-Bee CH, Kvasnak E, & Stehberg J (2008). Large-scale organization of rat sensorimotor cortex based on a motif of large activation spreads. J Neurosci 28, 13274-13284.

82.   Gabbott PL & Bacon SJ (1996). Local circuit neurons in the medial prefrontal cortex (areas 24a,b,c, 25 and 32) in the monkey: I. Cell morphology and morphometrics. J Comp Neurol 364, 567-608.

83.   Galarreta M & Hestrin S (1999). A network of fast-spiking cells in the neocortex connected by electrical synapses. Nature 402, 72-75.

84.   Gavrilovici C, D'Alfonso S, & Poulter MO (2010a). Diverse interneuron populations have highly specific interconnectivity in the rat piriform cortex. J Comp Neurol 518, 1570-1588.

85.   Gavrilovici C, D'Alfonso S, & Poulter MO (2010b). Diverse interneuron populations have highly specific interconnectivity in the rat piriform cortex. J Comp Neurol 518, 1570-1588.

86.   Gavrilovici C, D'Alfonso S, Dann M, & Poulter MO (2006). Kindling-induced alterations in GABAA receptor mediated inhibition and neurosteroid activity in the piriform cortex of rat. Eur J Neurosci 24, 1373-1384.

87.   George EB, Nyirjesy P, Basson M, Ernst LA, Pratap PR, Freedman JC, & Waggoner AS (1988). Impermeant potential-sensitive oxonol dyes: I. Evidence for an "on-off" mechanism. J Membr Biol 103, 245-253.

88.   Goddard GV, McIntyre DC, & Leech CK (1969). A permanent change in brain function resulting from daily electrical stimulation. Exp Neurol 25, 295-330.

89.   Gray CM, Konig P, Engel AK, & Singer W (1989). Oscillatory responses in cat visual cortex exhibit inter-columnar synchronization which reflects global stimulus properties. Nature 338, 334-337.

90.   Grinvald A & Farber IC (1981). Optical recording of calcium action potentials from growth cones of cultured neurons with a laser microbeam. Science 212, 1164-1167.

91.   Grinvald A, Fine A, Farber IC, & Hildesheim R (1983). Fluorescence monitoring of electrical responses from small neurons and their processes. Biophys J 42, 195-198.

92.   Grinvald A, Manker A, & Segal M (1982). Visualization of the spread of electrical activity in rat hippocampal slices by voltage-sensitive optical probes. J Physiol 333, 269-291.

93. Grinvald A, Ross WN, & Farber I (1981). Simultaneous optical measurements of electrical activity from multiple sites on processes of cultured neurons. Proc Natl Acad Sci U S A 78, 3245-3249.

94. Grinvald A, Salzberg BM, & Cohen LB (1977). Simultaneous recording from several neurones in an invertebrate central nervous system. Nature 268, 140-142.

95. Gross D & Loew LM (1989). Fluorescent indicators of membrane potential: microspectrofluorometry and imaging. Methods Cell Biol 30, 193-218.

96. Gross D, Loew LM, & Webb WW (1986). Optical imaging of cell membrane potential changes induced by applied electric fields. Biophys J 50, 339-348.

97. Gupta RK, Salzberg BM, Grinvald A, Cohen LB, Kamino K, Lesher S, Boyle MB, Waggoner AS, & Wang CH (1981). Improvements in optical methods for measuring rapid changes in membrane potential. J Membr Biol 58, 123-137.

98. Haas HL & Jefferys JG (1984). Low-calcium field burst discharges of CA1 pyramidal neurones in rat hippocampal slices. J Physiol 354, 185-201.

99. Haberly L & Behan M (1983). Structure of the piriform cortex of the opossum. III. Ultrastructural characterization of synaptic terminals of association and olfactory bulb afferent fibers. J Comp Neurol 219, 448-460.

100. Haberly LB & Bower JM (1984). Analysis of association fiber system in piriform cortex with intracellular recording and staining techniques. J Neurophysiol 51, 90-112.

101. Haberly LB & Feig SL (1983). Structure of the piriform cortex of the opossum. II. Fine structure of cell bodies and neuropil. J Comp Neurol 216, 69-88.

102. Haberly LB (1983). Structure of the piriform cortex of the opossum. I. Description of neuron types with Golgi methods. J Comp Neurol 213, 163-187.

103. Haberly LB, Hansen DJ, Feig SL, & Presto S (1987). Distribution and ultrastructure of neurons in opossum piriform cortex displaying immunoreactivity to GABA and GAD and high-affinity tritiated GABA uptake. J Comp Neurol 266, 269-290.

104. Hendry SH, Houser CR, Jones EG, & Vaughn JE (1983). Synaptic organization of immunocytochemically identified GABA neurons in the monkey sensory-motor cortex. J Neurocytol 12, 639-660.

105. Hestrin S & Galarreta M (2005). Electrical synapses define networks of neocortical GABAergic neurons. Trends Neurosci 28, 304-309.

106.	Heuschkel MO, Fejtl M, Raggenbass M, Bertrand D, & Renaud P (2002). A three-dimensional multi-electrode array for multi-site stimulation and recording in acute brain slices. J Neurosci Methods 114, 135-148.

107.	Hill DK & Keynes RD (1949). Opacity changes in stimulated nerve. J Physiol 108, 278-281.

108.	Hiyoshi T & Wada JA (1992). Lasting nature of both transfer and interference in amygdaloid kindling in cats: observation upon stimulation with 11-month rest following primary site kindling. Epilepsia 33, 222-227.

109.	Hotson JR & Prince DA (1980). A calcium-activated hyperpolarization follows repetitive firing in hippocampal neurons. J Neurophysiol 43, 409-419.

110.	Jack JJ (1975). Physiology of peripheral nerve fibres in relation to their size. Br J Anaesth 47 suppl, 173-182.

111.	Jimbo Y, Kawana A, Parodi P, & Torre V (2000). The dynamics of a neuronal culture of dissociated cortical neurons of neonatal rats. Biol Cybern 83, 1-20.

112.	Jobe PC, Picchioni AL, & Chin L (1973). Role of brain norepinephrine in audiogenic seizure in the rat. J Pharmacol Exp Ther 184, 1-10.

113.	Jones EG (1975). Varieties and distribution of non-pyramidal cells in the somatic sensory cortex of the squirrel monkey. J Comp Neurol 160, 205-267.

114.	Jones EG (1986). Neurotransmitters in the cerebral cortex. J Neurosurg 65, 135-153.

115.	Kahana MJ, Seelig D, & Madsen JR (2001). Theta returns. Curr Opin Neurobiol 11, 739-744.

116.	Kairiss EW, Racine RJ, & Smith GK (1984). The development of the interictal spike during kindling in the rat. Brain Res 322, 101-110.

117.	Kamino K, Katoh Y, Komuro H, & Sato K (1989). Multiple-site optical monitoring of neural activity evoked by vagus nerve stimulation in the embryonic chick brain stem. J Physiol 409, 263-283.

118.	Kamphuis W, De RT, & Lopes-da SF (1994). GABAA receptor □1-3 subunit gene expression in the hippocampus of kindled rats. Neurosci Lett 174, 5-8.

119.   Kanter ED & Haberly LB (1990). NMDA-dependent induction of long-term potentiation in afferent and association fiber systems of piriform cortex in vitro. Brain Res 525, 175-179.

120.   Kanter ED, Kapur A, & Haberly LB (1996). A dendritic GABAA-mediated IPSP regulates facilitation of NMDA-mediated responses to burst stimulation of afferent fibers in piriform cortex. J Neurosci 16, 307-312.

121.   Kapur A, Pearce RA, Lytton WW, & Haberly LB (1997). GABAA-mediated IPSCs in piriform cortex have fast and slow components with different properties and locations on pyramidal cells. J Neurophysiol 78, 2531-2545.

122.   Kashiwadani H, Sasaki YF, Uchida N, & Mori K (1999). Synchronized oscillatory discharges of mitral/tufted cells with different molecular receptive ranges in the rabbit olfactory bulb. J Neurophysiol 82, 1786-1792.

123.   Kawaguchi Y & Kondo S (2002). Parvalbumin, somatostatin and cholecystokinin as chemical markers for specific GABAergic interneuron types in the rat frontal cortex. J Neurocytol 31, 277-287.

124.   Kawaguchi Y & Kubota Y (1993). Correlation of physiological subgroupings of nonpyramidal cells with parvalbumin- and calbindinD28k-immunoreactive neurons in layer V of rat frontal cortex. J Neurophysiol 70, 387-396.

125.   Kawaguchi Y & Kubota Y (1997). GABAergic cell subtypes and their synaptic connections in rat frontal cortex. Cereb Cortex 7, 476-486.

126.   Kay LM & Freeman WJ (1998). Bidirectional processing in the olfactory-limbic axis during olfactory behavior. Behav Neurosci 112, 541-553.

127.   Klausberger T, Magill PJ, Marton LF, Roberts JD, Cobden PM, Buzsaki G, & Somogyi P (2003). Brain-state- and cell-type-specific firing of hippocampal interneurons in vivo. Nature 421, 844-848.

128.   Kobayashi M, Fujita S, Takei H, Song L, Chen S, Suzuki I, Yoshida A, Iwata K, & Koshikawa N (2010). Functional mapping of gustatory neurons in the insular cortex revealed by pERK-immunohistochemistry and in vivo optical imaging. Synapse 64, 323-334.

129.   Kopanitsa MV, Afinowi NO, & Grant SG (2006). Recording long-term potentiation of synaptic transmission by three-dimensional multi-electrode arrays. BMC Neurosci 7, 61.

130. Koplovitz I & Skvorak JP (1998). Electrocorticographic changes during generalized convulsive status epilepticus in soman intoxicated rats. Epilepsy Res 30, 159-164.

131. Laurent G (2002). Olfactory network dynamics and the coding of multidimensional signals. Nat Rev Neurosci 3, 884-895.

132. Lee KS, Schottler F, Collins JL, Lanzino G, Couture D, Rao A, Hiramatsu K, Goto Y, Hong SC, Caner H, Yamamoto H, Chen ZF, Bertram E, Berr S, Omary R, Scrable H, Jackson T, Goble J, & Eisenman L (1997). A genetic animal model of human neocortical heterotopia associated with seizures. J Neurosci 17, 6236-6242.

133. Leung LW & Yim CY (1991). Intrinsic membrane potential oscillations in hippocampal neurons in vitro. Brain Res 553, 261-274.

134. Lieke EE, Frostig RD, Arieli A, Ts'o DY, Hildesheim R, & Grinvald A (1989). Optical imaging of cortical activity: real-time imaging using extrinsic dye-signals and high resolution imaging based on slow intrinsic-signals. Annu Rev Physiol 51, 543-559.

135. Litaudon P, Datiche F, & Cattarelli M (1997). Optical recording of the rat piriform cortex activity. Prog Neurobiol 52, 485-510.

136. Litaudon P, Garcia S, & Buonviso N (2008). Strong coupling between pyramidal cell activity and network oscillations in the olfactory cortex. Neurosci 156, 781-787.

137. Loew LM & Simpson LL (1981). Charge-shift probes of membrane potential: a probable electrochromic mechanism for p-aminostyrylpyridinium probes on a hemispherical lipid bilayer. Biophys J 34, 353-365.

138. Loew LM, Bonneville GW, & Surow J (1978). Charge shift optical probes of membrane potential. Theory. Biochem 17, 4065-4071.

139. Loew LM, Cohen LB, Dix J, Fluhler EN, Montana V, Salama G, & Wu JY (1992). A naphthyl analog of the aminostyryl pyridinium class of potentiometric membrane dyes shows consistent sensitivity in a variety of tissue, cell, and model membrane preparations. J Membr Biol 130, 1-10.

140. Loew LM, Cohen LB, Salzberg BM, Obaid AL, & Bezanilla F (1985). Charge-shift probes of membrane potential. Characterization of aminostyrylpyridinium dyes on the squid giant axon. Biophys J 47, 71-77.

141. Loew LM, Scully S, Simpson L, & Waggoner AS (1979). Evidence for a charge-shift electrochromic mechanism in a probe of membrane potential. Nature 281, 497-499.

142.   Loscher W & Ebert U (1996a). Basic mechanisms of seizure propagation: targets for rational drug design and rational polypharmacy. Epilepsy Res Suppl 11, 17-43.

143.   Loscher W & Ebert U (1996b). The role of the piriform cortex in kindling. Prog Neurobiol 50, 427-481.

144.   Loscher W & Schmidt D (1994). Strategies in antiepileptic drug development: is rational drug design superior to random screening and structural variation? Epilepsy Res 17, 95-134.

145.   Lund JS (1984). Spiny stellate neurons. In Cerebral Cortex, eds. Peters A & Jones EG, pp. 255-308. Plenum Press, New York.

146.   Magee JC & Johnston D (1997). A synaptically controlled, associative signal for Hebbian plasticity in hippocampal neurons. Science 275, 209-213.

147.   Mann EO, Suckling JM, Hajos N, Greenfield SA, & Paulsen O (2005). Perisomatic feedback inhibition underlies cholinergically induced fast network oscillations in the rat hippocampus in vitro. Neuron 45, 105-117.

148.   Markram H, Lubke J, Frotscher M, & Sakmann B (1997). Regulation of synaptic efficacy by coincidence of postsynaptic APs and EPSPs [see comments]. Science 275, 213-215.

149.   Markram H, Toledo-Rodriguez M, Wang Y, Gupta A, Silberberg G, & Wu C (2004). Interneurons of the neocortical inhibitory system. Nat Rev Neurosci 5, 793-807.

150.   Martin C, Beshel J, & Kay LM (2007). An olfacto-hippocampal network is dynamically involved in odor-discrimination learning. J Neurophysiol 98, 2196-2205.

151.   Martinez MC, Blanco J, Bullon MM, & Agudo FJ (1987). Structure of the piriform cortex of the adult rat. A Golgi study. J Hirnforsch 28, 341-348.

152.   McBain CJ & Fisahn A (2001). Interneurons unbound. Nat Rev Neurosci 2, 11-23.

153.   McIntyre DC & Goddard GV (1973). Transfer, interference and spontaneous recovery of convulsions kindled from the rat amygdala. Electroencephalogr Clin Neurophysiol 35, 533-543.

154.   McIntyre DC & Molino A (1972). Amygdala lesions and CER learning: long term effect of kindling. Physiol Behav 8, 1055-1058.

155.   McIntyre DC & Plant JR (1993). Long-lasting changes in the origin of spontaneous discharges from amygdala-kindled rats: piriform vs. perirhinal cortex in vitro. Brain Res 624, 268-276.

156.   McIntyre DC, Poulter MO, & Gilby K (2002a). Kindling: some old and some new. Epilepsy Res 2002 Jun ;50 (1 -2):79 -92 50, 79-92.

157.   McIntyre DC, Poulter MO, & Gilby K (2002b). Kindling: some old and some new. Epilepsy Res 50, 79-92.

158.   Meldrum B & Horton R (1978). Blockade of epileptic responses in the photosesitive baboon, Papio papio, by 2 irreverrible inhibitors of GABA-transaminase, acetylinic GABA (4-amino-hex-5-ynoic acid) and vinyl GABA (4-amino-hex-5-enoic acid). Psychopharmacol 59, 47-50.

159.   Mennerick S, Chisari M, Shu HJ, Taylor A, Vasek M, Eisenman LN, & Zorumski CF (2010). Diverse voltage-sensitive dyes modulate $GABA_A$ receptor function. J Neurosci 30, 2871-2879.

160.   Mitzdorf U (1985). Current source-density method and application in cat cerebral cortex: investigation of evoked potentials and EEG phenomena. Physiol Rev 65, 37-100.

161.   Montana V, Farkas DL, & Loew LM (1989). Dual-wavelength ratiometric fluorescence measurements of membrane potential. Biochem 28, 4536-4539.

162.   Morgan JI & Curran T (1991). Proto-oncogene transcription factors and epilepsy. Trends Pharmacol Sci 12, 343-349.

163.   Nevander G, Ingvar M, Auer R, & Siesjo BK (1985). Status epilepticus in well-oxygenated rats causes neuronal necrosis. Ann Neurol 18, 281-290.

164.   Neville KR & Haberly LB (2004). The Synaptic Organization of the Brain Oxford University Press, New York.

165.   Obaid AL, Loew LM, Wuskell JP, & Salzberg BM (2004). Novel naphthylstyryl-pyridium potentiometric dyes offer advantages for neural network analysis. J Neurosci Methods 134, 179-190.

166.   Orbach HS & Cohen LB (1983). Optical monitoring of activity from many areas of the in vitro and in vivo salamander olfactory bulb: a new method for studying functional organization in the vertebrate central nervous system. J Neurosci 3, 2251-2262.

167.   Otto F, Gortz P, Fleischer W, & Siebler M (2003). Cryopreserved rat cortical cells develop functional neuronal networks on microelectrode arrays. J Neurosci Methods 128, 173-181.

168.   Parent JM, Janumpalli S, McNamara JO, & Lowenstein DH (1998). Increased dentate granule cell neurogenesis following amygdala kindling in the adult rat. Neurosci Lett 247, 9-12.

169.   Paxinos G & Watson PL (1986). The rat brain in stereotaxic coordinates, second ed. Academic Press, Syndey.

170.   Pedroarena C & Llinas R (1997). Dendritic calcium conductances generate high-frequency oscillation in thalamocortical neurons. Proc Natl Acad Sci U S A 94, 724-728.

171.   Petersen CC, Grinvald A, & Sakmann B (2003). Spatiotemporal dynamics of sensory responses in layer 2/3 of rat barrel cortex measured in vivo by voltage-sensitive dye imaging combined with whole-cell voltage recordings and neuron reconstructions. J Neurosci 23, 1298-1309.

172.   Piredda S & Gale K (1985). A crucial epileptogenic site in the deep prepiriform cortex. Nature 317, 623-625.

173.   Piredda S, Lim CR, & Gale K (1985). Intracerebral site of convulsant action of bicuculline. Life Sci 36, 1295-1298.

174.   Plenz D & Aertsen A (1993). Current source density profiles of optical recording maps: a new approach to the analysis of spatio-temporal neural activity patterns. Eur J Neurosci 5, 437-448.

175.   Pooler J (1972). Photodynamic alteration of sodium currents in lobster axons. J Gen Physiol 60, 367-387.

176.   Porter JT, Cauli B, Staiger JF, Lambolez B, Rossier J, & Audinat E (1998). Properties of bipolar VIPergic interneurons and their excitation by pyramidal neurons in the rat neocortex. Eur J Neurosci 10, 3617-3628.

177.   Porter LL & White EL (1986). Synaptic connections of callosal projection neurons in the vibrissal region of mouse primary motor cortex: an electron microscopic/horseradish peroxidase study. J Comp Neurol 248, 573-587.

178.   Poulter MO, Brown LA, Tynan S, Willick G, Williams R, & McIntyre DC (1999). Differential expression of alpha1, alpha2, alpha3, and alpha5 GABAA receptor

subunits in seizure-prone and seizure-resistant rat models of temporal lobe epilepsy. J Neurosci 19, 4654-4661.

179.   Princivalle A, Spreafico R, Bowery N, & de Curtis M (2000). Layer-specific immunocytochemical localization of GABA(B)R1a and GABA(B)R1b receptors in the rat piriform cortex. Eur J Neurosci 12, 1516-1520.

180.   Racine R, Tuff L, & Zaide J (1975). Kindling, unit discharge patterns and neural plasticity. Can J Neurol Sci 2, 395-405.

181.   Racine R., Steingert M.O., & McIntyre DC (1999). Development of kindling-prone and kindling-resistant rats: Selective breeding and electrophysiological studies. Epilepsy Res 35, 183-195.

182.   Racine RJ (1972a). Modification of seizure activity by electrical stimulation. II. Motor seizure. Electroencephalogr Clin Neurophysiol 32, 281-294.

183.   Racine RJ (1972b). Modification of seizure activity by electrical stimulation. I. After-discharge threshold. Electroencephalogr Clin Neurophysiol 32, 269-279.

184.   Racine RJ, Mosher M, & Kairiss EW (1988). The role of the pyriform cortex in the generation of interictal spikes in the kindled preparation. Brain Res 454, 251-263.

185.   Rall W & Shepherd GM (1968). Theoretical reconstruction of field potentials and dendrodendritic synaptic interactions in olfactory bulb. J Neurophysiol 31, 884-915.

186.   Ramón y Cajal S (1911). Histologie du Systéme Nerveux de l'Homme et des Vertébrés. Vol.II Maloine, Paris.

187.   Reers M, Smith TW, & Chen LB (1991). J-aggregate formation of a carbocyanine as a quantitative fluorescent indicator of membrane potential. Biochem 30, 4480-4486.

188.   Ren M, Yoshimura Y, Takada N, Horibe S, & Komatsu Y (2007). Specialized inhibitory synaptic actions between nearby neocortical pyramidal neurons. Science 316, 758-761.

189.   Ribak CE (1978). Aspinous and sparsely-spinous stellate neurons in the visual cortex of rats contain glutamic acid decarboxylase. J Neurocytol 7, 461-478.

190.   Ross WN, Salzberg BM, Cohen LB, & Davila HV (1974). A large change in dye absorption during the action potential. Biophys J 14, 983-986.

191. Ross WN, Salzberg BM, Cohen LB, Grinvald A, Davila HV, Waggoner AS, & Wang CH (1977). Changes in absorption, fluorescence, dichroism, and Birefringence in stained giant axons: : optical measurement of membrane potential. J Membr Biol 33, 141-183.

192. Rozov A, Jerecic J, Sakmann B, & Burnashev N (2001). AMPA receptor channels with long-lasting desensitization in bipolar interneurons contribute to synaptic depression in a novel feedback circuit in layer 2/3 of rat neocortex. J Neurosci 21, 8062-8071.

193. Sacks DS & Dasheiff RM (1992). In vivo mapping of drug-induced seizures with voltage-sensitive dye. Brain Res 595, 79-86.

194. Saggau P, Galvan M, & ten BG (1986). Long-term potentiation in guinea pig hippocampal slices monitored by optical recording of neuronal activity. Neurosci Lett 69, 53-58.

195. Salzberg BM, Grinvald A, Cohen LB, Davila HV, & Ross WN (1977). Optical recording of neuronal activity in an invertebrate central nervous system: simultaneous monitoring of several neurons. J Neurophysiol 40, 1281-1291.

196. Sato M, Racine RJ, & McIntyre DC (1990). Kindling: basic mechanisms and clinical validity. Electroencephalogr Clin Neurophysiol 76, 459-472.

197. Schnitzler A & Gross J (2005). Normal and pathological oscillatory communication in the brain. Nat Rev Neurosci 6, 285-296.

198. Schubert D, Kotter R, & Staiger JF (2007). Mapping functional connectivity in barrel-related columns reveals layer- and cell type-specific microcircuits. Brain Struct Funct 212, 107-119.

199. Schwartzkroin PA & Stafstrom CE (1980). Effects of EGTA on the calcium-activated afterhyperpolarization in hippocampal CA3 pyramidal cells. Science 210, 1125-1126.

200. Simon A, Olah S, Molnar G, Szabadics J, & Tamas G (2005). Gap-junctional coupling between neurogliaform cells and various interneuron types in the neocortex. J Neurosci 25, 6278-6285.

201. Sims PJ, Waggoner AS, Wang CH, & Hoffman JF (1974). Studies on the mechanism by which cyanine dyes measure membrane potential in red blood cells and phosphatidylcholine vesicles. Biochem 13, 3315-3330.

202.   Singer W (1999). Neuronal synchrony: a versatile code for the definition of relations? Neuron 24, 49-25.

203.   Sloviter RS (1987). Decreased hippocampal inhibition and a selective loss of interneurons in experimental epilepsy. Science 235, 73-76.

204.   Smiley ST, Reers M, Mottola-Hartshorn C, Lin M, Chen A, Smith TW, Steele GD, Jr., & Chen LB (1991). Intracellular heterogeneity in mitochondrial membrane potentials revealed by a J-aggregate-forming lipophilic cation JC-1. Proc Natl Acad Sci U S A 88, 3671-3675.

205.   Somogyi P & Soltesz I (1986). Immunogold demonstration of GABA in synaptic terminals of intracellularly recorded, horseradish peroxidase-filled basket cells and clutch cells in the cat's visual cortex. Neurosci 19, 1051-1065.

206.   Somogyi P, Freund TF, Hodgson AJ, Somogyi J, Beroukas D, & Chubb IW (1985). Identified axo-axonic cells are immunoreactive for GABA in the hippocampus and visual cortex of the cat. Brain Res 332, 143-149.

207.   Steriade M (2001). Impact of network activities on neuronal properties in corticothalamic systems. J Neurophysiol 86, 1-39.

208.   Strogatz SH, Mirollo RE, & Matthews PC (1992). Coupled nonlinear oscillators below the synchronization threshold: Relaxation by generalized Landau damping. Phys Rev Lett 68, 2730-2733.

209.   Sugitani M, Sugai T, Tanifuji M, & Onoda N (1994b). Signal propagation from piriform cortex to the endopiriform nucleus in vitro revealed by optical imaging. Neurosci Lett 171, 175-178.

210.   Sugitani M, Sugai T, Tanifuji M, Murase K, & Onoda N (1994a). Optical imaging of the in vitro guinea pig piriform cortex activity using a voltage-sensitive dye. Neurosci Lett 165, 215-218.

211.   Suzuki N & Bekkers JM (2007). Inhibitory interneurons in the piriform cortex. Clin Exp Pharmacol Physiol 34, 1064-1069.

212.   Szentagothai J & Arbib MA (1974). Conceptual models of neural organization. Neurosci Res Program Bull 12, 305-510.

213.   Tamas G, Buhl EH, Lorincz A, & Somogyi P (2000). Proximally targeted GABAergic synapses and gap junctions synchronize cortical interneurons. Nat Neurosci 3, 366-371.

214.   Tasaki I, Watanabe A, Sandlin R, & Carnay L (1968). Changes in fluorescence, turbidity, and birefringence associated with nerve excitation. Proc Natl Acad Sci U S A 61, 883-888.

215.   Taylor CP & Dudek FE (1984). Excitation of hippocampal pyramidal cells by an electrical field effect. J Neurophysiol 52, 126-142.

216.   Thomson AM (2003). Presynaptic frequency- and pattern-dependent filtering. J Comput Neurosci 15, 159-202.

217.   Tominaga T, Tominaga Y, Yamada H, Matsumoto G, & Ichikawa M (2000). Quantification of optical signals with electrophysiological signals in neural activities of Di-4-ANEPPS stained rat hippocampal slices. J Neurosci Methods 102, 11-23.

218.   Tominaga Y, Ichikawa M, & Tominaga T (2009). Membrane potential response profiles of CA1 pyramidal cells probed with voltage-sensitive dye optical imaging in rat hippocampal slices reveal the impact of GABA(A)-mediated feed-forward inhibition in signal propagation. Neurosci Res 64, 152-161.

219.   Traub RD, Jefferys JGR, & Whittington MA (1999). Fast Oscillations in Cortical Circuits MIT Press.

220.   Tsien RY & Hladky SB (1978). A quantitative resolution of the spectra of a membrane potential indicator, diS-C3-(5), bound to cell components and to red blood cells. J Membr Biol 38, 73-97.

221.   Ts'o DY, Frostig RD, Lieke EE, & Grinvald A (1990). Functional organization of primate visual cortex revealed by high resolution optical imaging. Science 249, 417-420.

222.   Turski L, Ikonomidou C, Turski WA, Bortolotto ZA, & Cavalheiro EA (1989). Review: cholinergic mechanisms and epileptogenesis. The seizures induced by pilocarpine: a novel experimental model of intractable epilepsy. Synapse 3, 154-171.

223.   Turski WA, Cavelheiro EA, Schwartz M, Czuczwar SJ, Kleinrok Z, & Turski L (1983). Limbic seizures produced by pilocarpine in rats: behavioural, electroencephalographic and neuropathological study. Behav Brain Res 9, 315-335.

224.   Varela F, Lachaux JP, Rodriguez E, & Martinerie J (2001). The brainweb: phase synchronization and large-scale integration. Nat Rev Neurosci 2, 229-239.

225.   Verney C, Alvarez C, Geffard M, & Berger B (1990). Ultrastructural Double-Labelling Study of Dopamine Terminals and GABA-Containing Neurons in Rat Anteromedial Cerebral Cortex. Eur J Neurosci 2, 960-972.

226.   von WG, Avrabos C, Stepan J, Wurst W, Deussing JM, Holsboer F, & Eder M (2011). Voltage-sensitive dye imaging demonstrates an enhancing effect of corticotropin-releasing hormone on neuronal activity propagation through the hippocampal formation. J Psychiatr Res 45, 256-261.

227.   Waggoner AS & Grinvald A (1977). Mechanisms of rapid optical changes of potential sensitive dyes. Ann N Y Acad Sci 303, 217-241.

228.   Waggoner AS (1979). Dye indicators of membrane potential. Annu Rev Biophys Bioeng 8, 47-68.

229.   Waggoner AS (1988). Mechanisms of membrane potential probes. Soc Gen Physiol Ser 43, 209-215.

230.   Walton NY & Treiman DM (1988). Experimental secondarily generalized convulsive status epilepticus induced by D,L-homocysteine thiolactone. Epilepsy Res 2, 79-86.

231.   White EL & Hersch SM (1981). Thalamocortical synapses of pyramidal cells which project from SmI to MsI cortex in the mouse. J Comp Neurol 198, 167-181.

232.   White EL & Hersch SM (1982). A quantitative study of thalamocortical and other synapses involving the apical dendrites of corticothalamic projection cells in mouse SmI cortex. J Neurocytol 11, 137-157.

233.   Whittington MA & Traub RD (2003). Interneuron diversity series: inhibitory interneurons and network oscillations in vitro. Trends Neurosci 26, 676-682.

234.   Wirth C & Luscher HR (2004). Spatiotemporal evolution of excitation and inhibition in the rat barrel cortex investigated with multielectrode arrays. J Neurophysiol 91, 1635-1647.

235.   Wollner DA & Catterall WA (1986). Localization of sodium channels in axon hillocks and initial segments of retinal ganglion cells. Proc Natl Acad Sci U S A 83, 8424-8428.

236.   Wong RK, Prince DA, & Basbaum AI (1979). Intradendritic recordings from hippocampal neurons. Proc Natl Acad Sci U S A 76, 986-990.

237.   Woolsey TA & Van der Loos H (1970). The structural organization of layer IV in the somatosensory region (SI) of mouse cerebral cortex. The description of a cortical field composed of discrete cytoarchitectonic units. Brain Res 17, 205-242.

238.   Yae H, Elias SA, & Ebner TJ (1992). Deblurring of 3-dimensional patterns of evoked rat cerebellar cortical activity: a study using voltage-sensitive dyes and optical sectioning. J Neurosci Methods 42, 195-209.

239.   Ylinen A, Bragin A, Nadasdy Z, Jando G, Szabo I, Sik A, & Buzsaki G (1995a). Sharp wave-associated high-frequency oscillation (200 Hz) in the intact hippocampus: network and intracellular mechanisms. J Neurosci 15, 30-46.

240.   Ylinen A, Soltesz I, Bragin A, Penttonen M, Sik A, & Buzsaki G (1995b). Intracellular correlates of hippocampal theta rhythm in identified pyramidal cells, granule cells, and basket cells. Hippocampus 5, 78-90.

241.   Zibrowski EM & Vanderwolf CH (1997). Oscillatory fast wave activity in the rat pyriform cortex: relations to olfaction and behavior. Brain Res 766, 39-49.